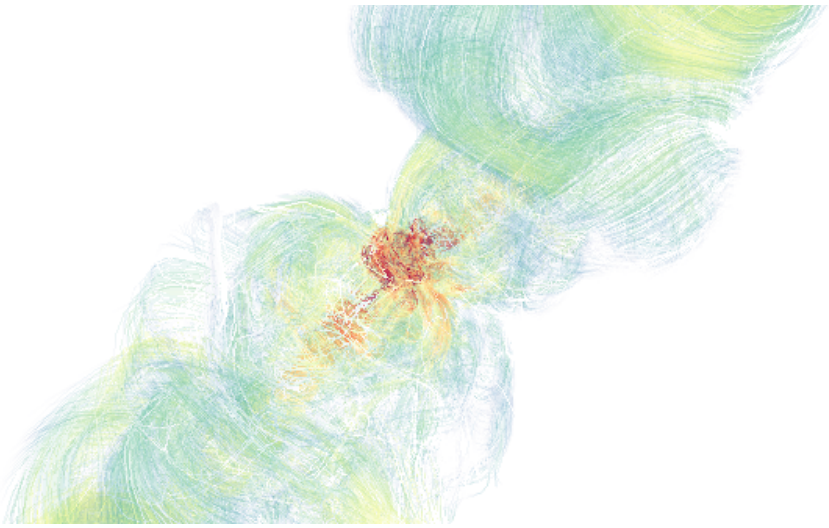

Supernovae: rotation and magnetic fields

Prelude: what do we observe in stars?

Rotation in the Sun and massive stars

Rotation and magnetic fields are omnipresent in the Universe and have been found from the Sun and the Solar System to galactic scales and beyond. The solar surface rotation with a period of of about 27 days is directly visible in the motion of sunspots. Without the ability to spatially resolve the surface of other stars, their rotational velocities of the photospheres can be inferred spectroscopically via the Doppler effect. For massive stars, including the potential progenitors of core-collapse supernovae (CCSNe), surface rotation with velocities of several $100\,\mathrm{km/s}$ have been found. Such values correspond to significant fractions of the critical rotational velocity, $v_{\mathrm{crit}}^2 = \Omega_{\mathrm{crit}}^2 R_{\star,\mathrm{crit}}^2 = \frac{GM_\star}{R_{\star,\mathrm{crit}}} = \frac{2GM_\star}{3R_{\star,\mathrm{crit}}}$, at which the centrifugal forces exceed gravity, corresponding to the mass-shedding limit. Helio-/asteroseismology can give us information about the rotational profile inside the photosphere. Typically, stars do not rotate as a rigid body. The internal rotational profile of the Sun has been mapped down to about half its radius. Latitudinal differential rotation is present at the surface and in the (upper) convective layer. It transitions to rigid rotation below that in a region of radial differential rotation, the tachocline.

https://prod-files-secure.s3.us-west-2.amazonaws.com/7dc393d7-041f-4dad-abb2-7743053e06ac/c5fadecd-9372-4bf5-9da7-43f3da6dc45a/solar_rotation.mp4

Visualisation of the solar rotation. Source: NASA, https://solarsystem.nasa.gov/solar-system/sun/overview/

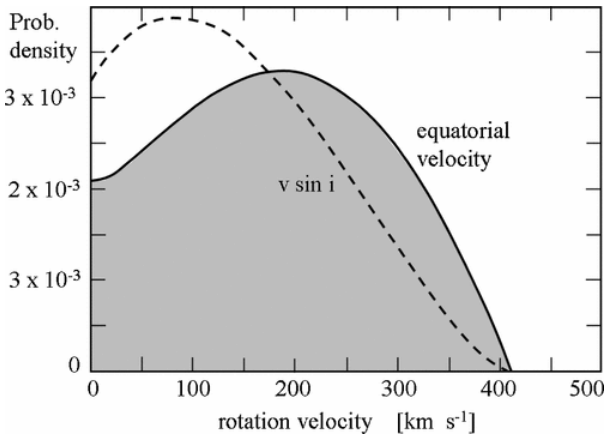

Probability density of rotation velocities for 496 stars of spectral types from O9.5 to B8 (masses 3 - 20 M_sol). From Huang & Gies (2006, http://dx.doi.org/10.1086/505782).

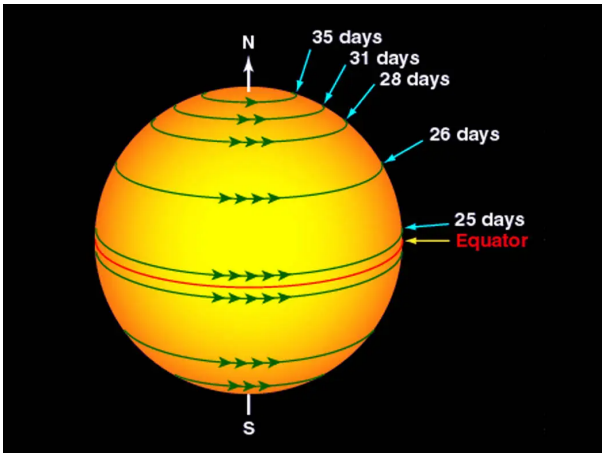

Differential rotation at the solar surface. https://www.nasa.gov/image-article/solar-rotation-varies-by-latitude/

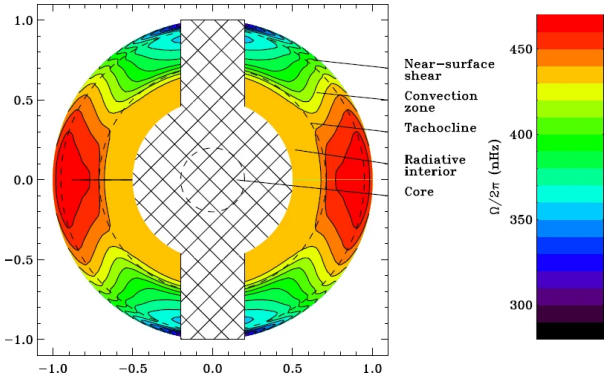

Internal differential rotation of the Sun as inferred from the Michelson Doppler Instrument (MDI) aboard the SOHO spacecraft (Howe, 2099, https://link.springer.com/article/10.12942/lrsp-2009-1).

Magnetic fields

Evidence for magnetic fields in the Sun and stars comes from several classes of observations:

- Satellites can use sensors to probe the fields of the solar wind in situ.
- Imaging (e.g., Halpha, UV) of the solar surface and corona reveals structures following magnetic field lines.
- Polarisation measurements can be used to infer strength and orientation of the field.
    - Zeeman effect: measurement of splitting of suitable spectral lines in an external magnetic field, $\propto |\vec{B}|$. Longitudinal and transversal Zeeman effect lead to circular and linear

polarisation, respectively.

    - Hanle effect: polarisation of scattered light, useful for weak and small-scale fields.
    - Faraday effect: rotation of the polarisation of linearly polarised light, $\propto |B_{\parallel}|$.
- Synchrotron emission of charged particles in a magnetic field, $\propto |\vec{B}|$.

The precise origin of the Sun's rotational profile is still a matter of investigation. What is clear is that rotation, convection, and magnetic fields are closely related. Differential rotation and convection can amplify a seed magnetic field, and the magnetic field as well as convective eddies can redistribute angular momentum. The resulting solar magnetic field is complex and varies with times. It can be described as the superposition of two components:

1. A large-scale dipole field whose strength and orientation varies over the course of the 22 year solar cycle extends far beyond the solar surface. It is at 10 G relatively weak.
2. Rapidly varying fields on a wide range of length scales from a significant fraction of the solar radius down to the diameters of sunspots, granulation cells, and below. These fields can be > 3 orders of magnitude stronger than the dipole. They are particularly strong at sunspots. They drive much of the solar activity (flares, coronal mass ejections) and may be behind the heating of the corona to $T_{\mathrm{corona}} \sim \mathcal{O}(10^6\,\mathrm{K}) \gg T_{\mathrm{photosphere}} \sim 5600\,\mathrm{K}$.

Despite the vastly different length and time scales, the two classes of fields are linked, as can be inferred from the sunspot-related small-scale fields and the associated activity following the same cycle as the dipole field. How they are generated and how the properties of the cycle are set, is still a field with many open questions. The small-scale fields are clearly related to the convective cells, but how they connect to the large-scale field and its long-term quasi-periodicity is less clear. In any case, the solar field is an example of a dynamo, i.e., a system in which a magnetic field is amplified or, after an initial phase of amplification, maintained against processes that would otherwise lead to its dissipation.

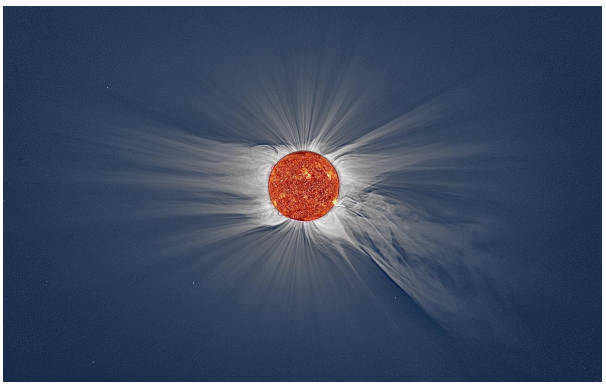

The white regions surrounding the solar disk image show the solar corona photographed in visible light during the 2021 total solar eclipse. The solar disk image taken from the SDO space telescope shows the upper chromosphere. Credit: Miloslav Druckmüller, Andreas Möller, SDO AIA 30.4
nm. https://www.iac.es/en/outreach/news/novel-code-exploring-magnetic-field-solar-corona

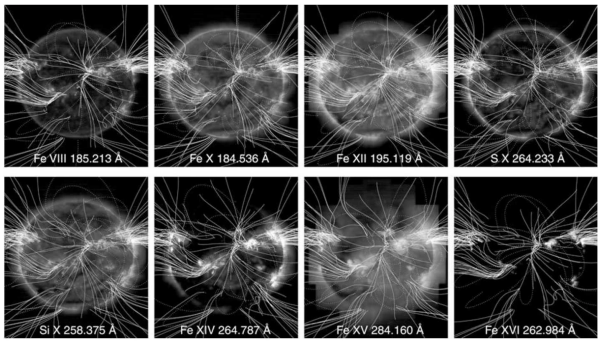

Magnetic fields lines from a potential field source surface (PFSS) calculation are overlaid on the full-Sun intensity images from Hinode-EIS. The solid lines are open and the dotted lines are closed. Each pixel in these images has a spectrum which allows the Doppler velocity and abundance to be determined, and the regions corresponding to sources of solar wind to be determined (Brooks et al. 2015).

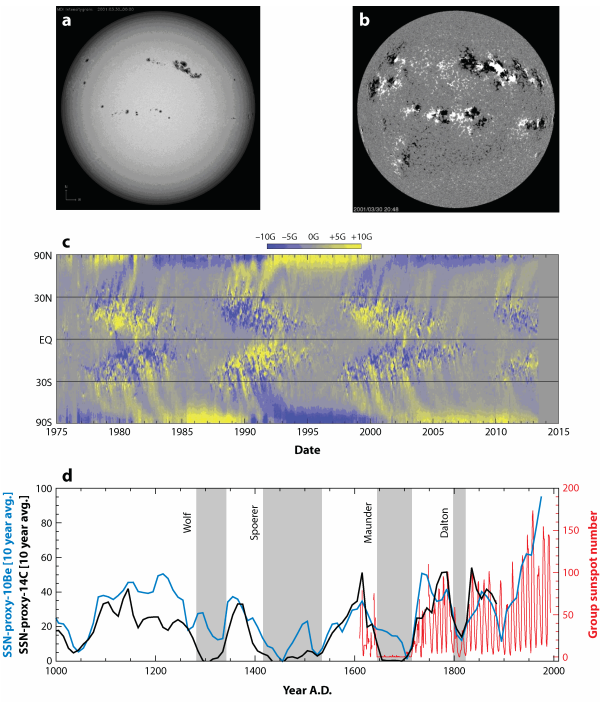

Charbonneau P. 2014.
Annu. Rev. Astron. Astrophys. 52:251–90

Solar magnetic field:
Panels a (continuum light) and b (magnetogram) show groups of sunpots and the magnetic fields associated to them.
Panel c (butterfly diagram) shows the time evolution of the solar magnetic field with over several 11/22 year cycles.
Panel d: time series of sun spot numbers as proxies for solar activity.
Source: Charbonneau (2014, https://www.annualreviews.org/content/journals/10.1146/astro-081913-040012)

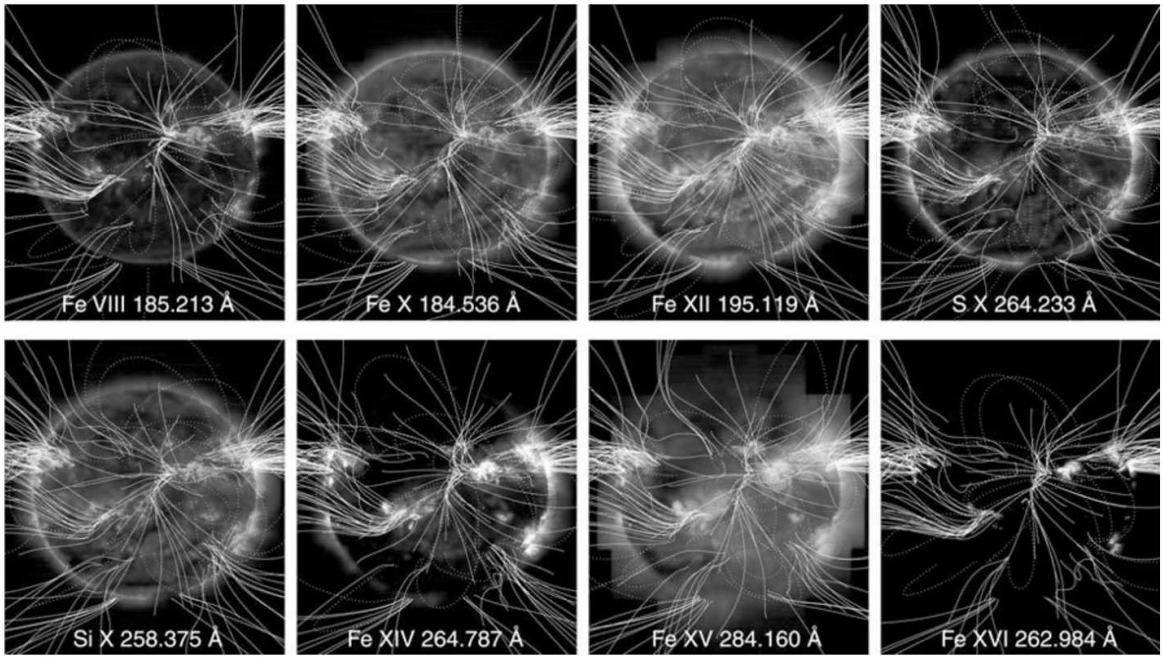

Stars similar to the Sun (in the sense of having a subsurface convection zone) show similar activity patterns indicating the presence of a magnetic field. Massive main-sequence stars, powered by H-burning via the CNO cycle rather than the pp-chain, have convective cores and radiative outer layers. Evidence for strong large-scale surface fields is limited (of order 10 %) and possibly connected to stars formed by mergers in close binaries. Note that, as far as CCSNe are concerned, the surface fields are less relevant than the ones in the core.

Some basics on rotation and magnetic fields

Rotation

The angular momentum, $\vec{J} = \rho \vec{r} \times \vec{v}$ (in spherical coordinates for rotation about the z-axis, $J_z = \rho r \sin\theta v_\phi$), is a conserved quantity, at least when integrated over the entire Universe. At the local level, angular momentum can be transported between fluid elements, e.g., by fluid stresses or magnetic fields. In the absence of such transport, contraction of a body leads to a spin-up and increase of the rotational energy, while expansion reduces the angular velocity. The former applies, e.g., to the core collapse at the end of the stellar life, the latter can cause stars to lose rotational energy in winds.

Rotation affects the structure and evolution of a star or stellar core via the Coriolis and the centrifugal force. The former is more subtle, the latter has several direct impacts:

- $F_c = r \sin\theta \, \Omega^2$ counteracts gravity. Thus, the centrifugal force can help stabilise a star against gravity. This effect can be important for rapidly rotating neutron stars as it can allow them to exist at masses above the (EOS-dependent) TOV limit for non-rotating objects.
- Being strongest at the equator, the centrifugal force can flatten a star into an oblate shape.

- For very rapid rotation, it can support gas against gravity even in the absence of pressure. In the gravitational force of a point mass, the result can be Keplerian rotation, $\Omega \propto r^{-3/2}$ and the formation of a disc.
- Still faster rotation may lead to mass shedding or the breakup of the object.

How important the effects of rotation on the structure are can be estimated using the ratio between rotational and gravitational energy of the star, $T/|W|$. Hydrodynamic instabilities can set in even at values $T/|W| \sim \mathcal{O}(0.01 - 0.1)$. Examples are bar mode deformations which can be quite effective at transporting angular momentum from the centre outward. The effect of rotation tends to be enhanced if, for the same $T/|W|$, the star rotates differentially with $\partial_r \Omega < 0$.

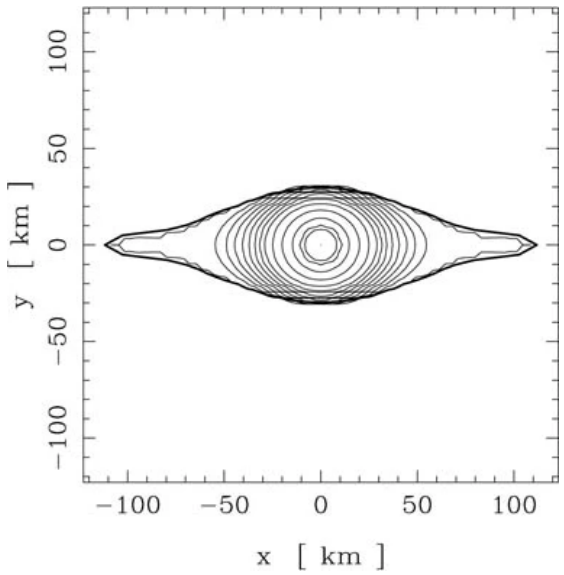

Iso-energy density lines of a differentially rotating proto-neutron star at the mass-shedding limit (Goussard et al., 1997). https://link.springer.com/article/10.12942/lrr-2003-3

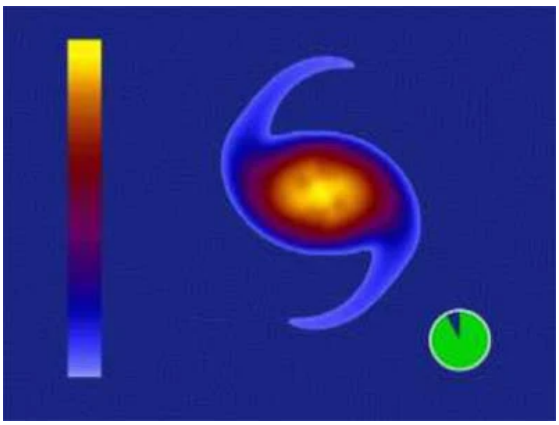

Still from a movie showing the development of the dynamical barmode instability in a rapidly rotating relativistic star. Spiral arms form within a few rotational periods. The different colors correspond to different values of the density, while the computation was done in full general relativity. http://www.physics.uiuc.edu/, https://link.springer.com/article/10.12942/lrr-2003-3

Magnetic fields

→ see Spruit (2013)

Induction equation and Lorentz force

In the framework of magnetohydrodynamics (MHD), the magnetic field evolves according to the induction equation, $\partial_t \vec{B} = -\vec{\nabla} \times \vec{E}$. Irrespective of the form of the electric field $\vec{E}$, we can note:

1. If $\vec{\nabla} \cdot \vec{B} = 0$ initially (no sources/sinks of magnetic field, i.e., magnetic monopoles), it remains so forever. While this constraint is true analytically, numerical schemes have to be designed such as to satisfy it.

2. By virtue of Stokes' theorem, the induction equation amounts to a conservation law for the magnetic flux through a surface area, $\Phi_A = \int_A d\vec{A} \cdot \vec{B}$.

The magnetic field can be described by magnetic field lines, which (zero divergence) have no beginning or end. If we can assume infinite electric conductivity, which is not a bad assumption in stellar interiors, the electric field is given by the velocity and the magnetic field, and we get the induction equation of ideal MHD, $\partial_t \vec{B} = \vec{\nabla} \times (\vec{v} \times \vec{B})$. A prescribed velocity field can modify a magnetic field by compressing or expanding the field lines or by bending them. In ideal MHD, field lines move together with the gas: a magnetic field line passing through an infinitesimal fluid element will always remain attached to it - the magnetic flux is frozen into the gas. A fluid element can, however, slide along a field line.

The magnetic field exerts the Lorentz force $\vec{F}_\mathrm{L} = \frac{1}{4\pi}(\vec{\nabla} \times \vec{B}) \times \vec{B}$ on the gas, always orthogonal to the magnetic field. It can be written as the sum of two contributions, $\vec{F}_\mathrm{L} = \vec{F}_\mathrm{L,p} + \vec{F}_\mathrm{L,c}$:

1. The magnetic pressure force, $\vec{F}_\mathrm{L,p} = -\frac{1}{8\pi}\vec{\nabla}_\perp B^2$ ($\vec{\nabla}_\perp$ is the projection of $\vec{\nabla}$ perpendicular to the magnetic field) describes a force loosely analogous to the pressure of a gas, though acting only perpendicular to the field lines. If no other force were at work, the pressure force would make the magnetic field strength, or, equivalently, the magnetic pressure $P_\mathrm{m} = B^2/8\pi$, uniform. In the picture of field lines, the magnetic pressure corresponds to the density of field lines.
2. The magnetic curvature force, $\vec{F}_\mathrm{L,c} = +\frac{B^2}{4\pi}\vec{s} \cdot \vec{\nabla}\vec{s}$, is also perpendicular and directed along the normal vector to the field line, $\vec{n} = (\vec{s} \cdot \vec{\nabla})\vec{s}$, where $\vec{s} = \vec{B}/B$ denotes the tangential vector. It is inversely proportional to the curvature radius of a field line, $\propto R_\mathrm{c}^{-1}$, thus vanishing for any straight field line. It would, by itself, make a field line as straight and short as possible.

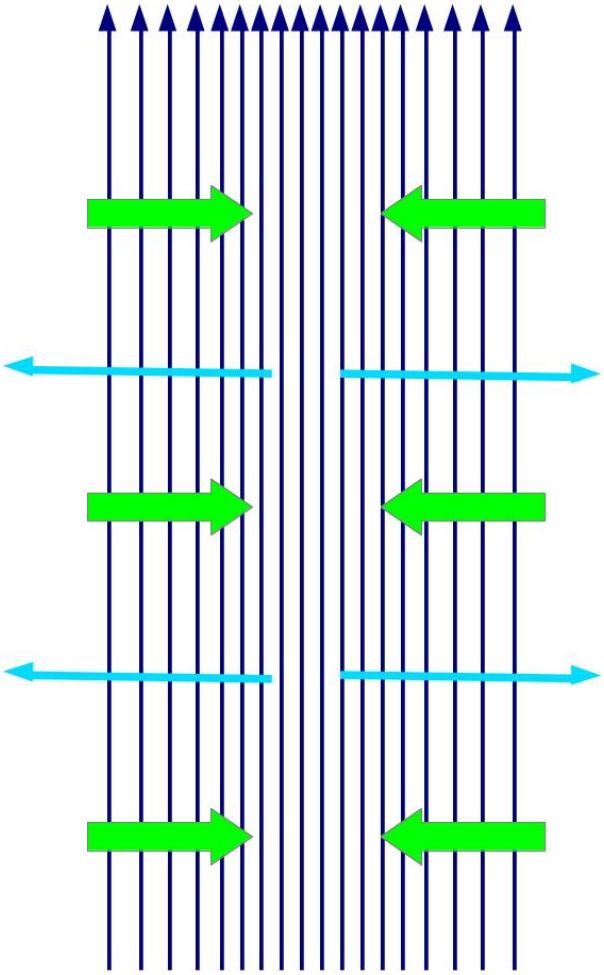

Field lines of an inhomogeneous magnetic field. The Lorentz force (blue arrows) is directed from regions of high magnetic pressure (dense field lines) to lower pressure. The green arrows represent a converging velocity field that could compress the field lines to such a state.

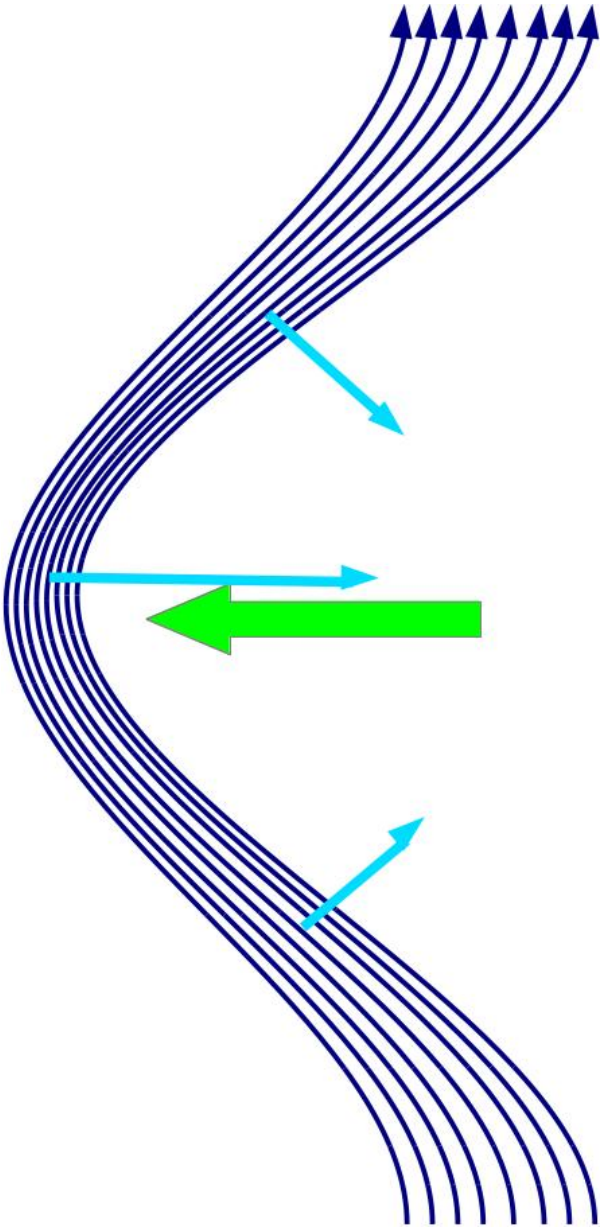

A magnetic field that has been bent into a state of non-zero curvature by the velocity shown with the green arrow. The Lorentz force (blue) would restore a straight magnetic field.

The curvature force has an important consequence for a rotating plasma. Imagine two fluid elements rotating at different angular velocities that are connected by a field line. The field line can be straight, i.e., have vanishing curvature, if the two fluid elements rotate at the same angular velocity. Hence, the magnetic field has the tendency to enforce rigid rotation along a field line. This process correpsonds to a transport of angular momentum along the field lines. If the star rotates faster in the centre than outside, then the transport occurs in the outward direction.

The Lorentz force allows for wave-like solutions, which add complexity to the sound waves of hydrodynamics:

- The curvature force gives rise to transverse Alfvén waves propagating at the Alfvén speed, $c_\mathrm{A} = |B|/(\sqrt{4\pi\rho})$ (approximately, the actual speed depends on the orientation w.r.t. the field lines.
- The compressional sound wave splits into a slow and a fast magnetosonic wave. Their speed is approximately (again direction-dependent) $c_\mathrm{f,s} = c_\mathrm{snd} \pm c_\mathrm{A}$.

The Lorentz force can, via the work done, transfer energy between the gas and the magnetic field. Compressing or bending field lines requires overcoming the Lorentz force and thus increases the energy density of the magnetic field, $e_\mathrm{m} = B^2/8\pi$, i.e., amplifies the field strength, at the expense of the kinetic energy of the fluid. An expansion of the field or the straightening of the field lines accelerates the gas and transfers energy the other way round. Whether in a given system the gas or the magnetic field dominates the dynamics, can often be assessed by comparing the magnetic pressure (or equivalently, energy density) to the gas pressure (using the plasma-beta parameter $\beta = P/P_\mathrm{m}$) or to the kinetic energy density. Usually, if the gas dominates, the field follows its motion, often leading to field amplification; in the opposite case, the field determines where the gas has to go. Alternatively, one can compare the Alfvén speed to flow and sound speed to see how important the magnetic field is w.r.t. the gas velocity and the internal energy/gas pressure.

While the conductivity of stellar plasmas is enormous, it is not strictly infinite. The resistivity, the inverse of the conductivity, of the gas can lead to a gradual dissipation of the currents carrying the magnetic field. Thus, the magnetic energy will slowly weaken. As a side note, the dynamics of resistive MHD is very rich, as the consequences of a finite resistivity go beyond a gradual dissipation of the field and include the reconnection of magnetic field lines, possibly via instabilities. Intense reconnection, e.g., in solar flares or magnetised (GRB) jets, can lead to the acceleration of charged particles to high energies.

In our context, a dynamo is a mechanism, flow field, etc that can amplify a weak seed field or, after the amplification saturates, maintain its strength and energy against (resistive) dissipation and the backreaction of the Lorentz force. Dynamos are often driven by hydrodynamic/hydromagnetic instabilities (Kelvin-Helmholtz, Rayleigh-Taylor, ...) and the ensuing turbulent velocity field in which small-scale vortices stretch, twist, and fold the field lines. Typical examples can be found in the convective zone of the Sun. Turbulent dynamos usually lead to a wide spectrum of length scales / wave numbers in the magnetic field. We can distinguish between

- small-scale dynamos: the magnetic field is dominated by the same length scales as the turbulent velocity field;
- large-scale dynamos: the small-scale magnetic field generated by the turbulent motion rearranges itself in such a way that the energy is transmitted to larger and larger spatial scales, e.g., a global dipole field. For that to happen, special conditions are necessary, commonly in the form of rotation.

In rotating stars, differential rotation can wind up a poloidal (radial and latitudinal components) field into a toroidal one (in the longitudinal ϕ-direction) and thereby amplify the total field strength (the Ω effect). Turbulent motions of v_r and v_θ depending on ϕ can close the loop by generating a poloidal field from the toroidal component (α effect). In line with various anti-dynamo theorems, the resulting $\alpha - \Omega$ dynamo is only possible in three dimensions without any, e.g., axial, symmetry.

The saturation level of the dynamo-generated magnetic field is often set by the local equipartition between kinetic and magnetic energy density as that is the point at which the Lorentz force can resist further compression or bending of field lines, thus quenching the dynamo.

Rotation and magnetic fields: spin down

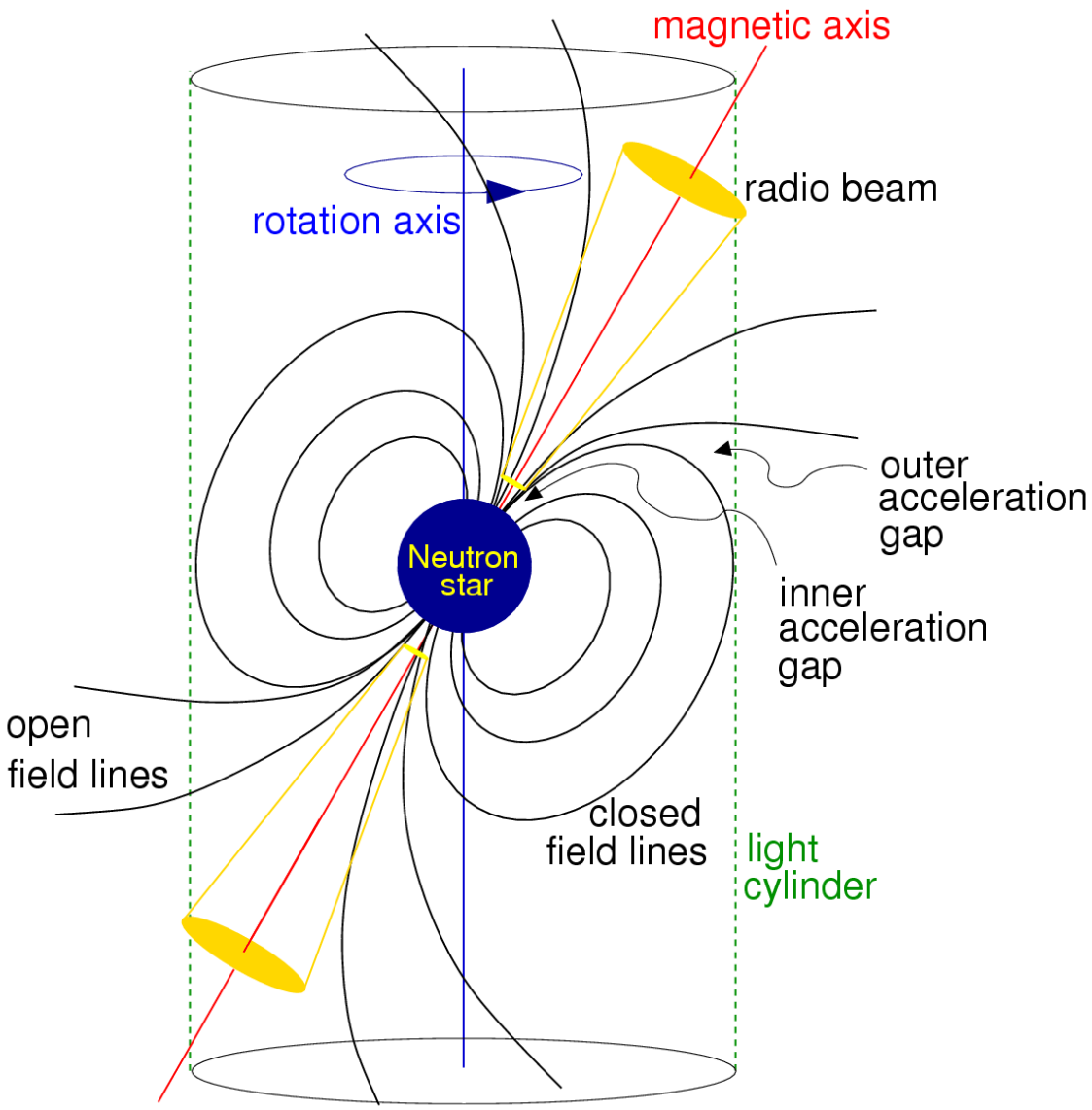

Schematic of a pulsar as a spinning neutron star with an inclined dipole magnetic field.

Assume a star in vacuum, endowed with a dipole magnetic field of strength B inclined by an angle α w.r.t. the axis around which it rotates with angular velocity Ω and period P. The time-dependent dipole moment will lead to the emission of energy in the form of electromagnetic radiation with a power of $P_{\rm rad} = \frac{2\ddot{p}_\perp^2}{3c^3} = ... = \frac{2}{3c^3} m_\perp^2 \Omega^4 = \frac{2}{3c^3} \left(BR^3 \sin\alpha\right)^2 (2\pi/P)^4$, where $p_\perp, m_\perp$ are the perpendicular component of the electric, magnetic dipole moments, respectively, R is the radius of the star. The energy source of the radiation is the rotational energy, $E_{\rm rot} = I\Omega^2/2 = 2\pi^2 I/P^2$ ($I = \frac{2}{5}MR^2$ is the inertial moment), which is lost at a rate $\dot{E}_{\rm rot} = -\frac{4\pi^2 I\dot{P}}{P^3}$. We can combine the

energy loss and the radiative power and find an expression for the rate of change of the period: $\dot{P} = \frac{8\pi^2 R^6 \sin^2 \alpha B^2}{3c^3 I P}$.

The stronger the magnetic field, the faster the spin-down. In the case of pulsars, the rate of change of the rotational energy can be of the order of $10^5 L_\odot$ (values for the Crab pulsar).

While the basic idea of a magnetic field mediating the spin-down of a rapidly rotating object and thus serving to liberate energy at large rates, is applicable to many astrophysical systems, including, as we shall see below, supernovae, the simple sketch here has to be modified in many cases. The star may not be in vacuum, but surrounded by more or less dense matter subject to many other forces and processes relevant to the dynamics; the dipole configuration may be too simplistic a description for the true magnetic field, which, additionally, may be varying with time.

Magnetic fields and rotation in SN progenitors

For determining the pre-collapse state of an SN progenitor, one-dimensional hydrostatic stellar evolution modelling in spherical symmetry with a few additional assumptions is the main tool as the long time scales from star formation to collapse restrict the use of multi-dimensional dynamic models. Its main ingredients are

1. The equations of hydrostatic equilibrium for a self-gravitating (almost) spherical body.
2. Nuclear burning generating internal energy and converting light elements into heavier ones.
3. Transport of energy by radiation (diffusion) to the stellar surface.
4. Simplified models for (genuinely multi-dimensional and dynamic) convection (mixing-length theory, ...) and other flows that add to the transport of energy and can mix nuclear species. This is a major source of uncertainty in current theory.
5. In a similar vein, simplified recipes for the transport rotation and magnetic fields, including models for instability-driven dynamos and the (magnetic) transport of angular momentum.
6. Mass loss via winds or pulsations, described in approximate ways.
7. Approximate ways to include effects of binarity, e.g., mass transfer.

Many of these prescriptions have to be calibrated based on observations or theory. Numerical models in this framework can well reproduce the evolution of stars across the HRD by computing a series of equilibrium models taking into account the gradual changes of mass, composition etc due to nuclear burning, winds and other effects. In that way it is possible to construct large sets of stars across the range of SN progenitor masses, metallicities, and rotation rates. Radial profiles of density, temperature, composition, radial and rotational velocity, in the final state, i.e., the loss of hydrostatic equilibrium right before the collapse, are used as initial conditions for CCSN models.

Current models commonly include a model for the Tayler-Spruit dynamo operating in radiative, i.e., convectively stable, zones (e.g., https://ui.adsabs.harvard.edu/abs/2005ApJ...626..350H/abstract). It is based on a dynamo loop constituted by the instability of a toroidal field and differential rotation. Models of this kind predict a non-zero magnetic field in radiative zones, while leaving

convective layers devoid of magnetic field. The toroidal and poloidal components yield a rate at which angular momentum is transported.

The precise profiles of magnetic fields and rotation given by these models are sensitive to the progenitor mass, the formulations used to approximate the multi-dimensional and dynamic processes, including the choice of parameters and calibrations. A common result is a spin-down of the star over its hydrostatic evolutionary phases, in particular for strong mass loss. The final magnetisation tends to be moderate. It is possible for rotation to lead to enhanced mixing of chemical species on the main sequence, which has an influence on the core masses and, in consequence, on the explosion dynamics.

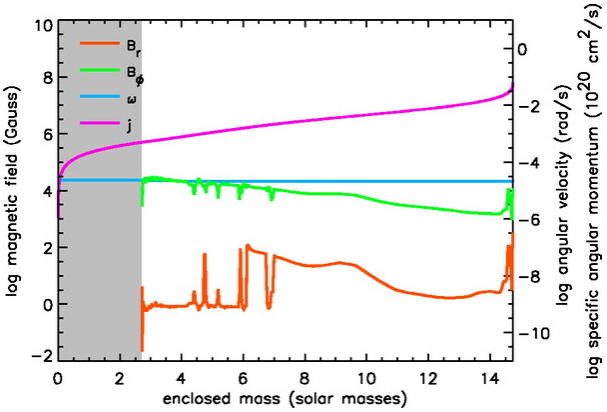

Structure of a 15 solar-mass star computed in 1d stellar evolution using the Tayler-Spruit dynamo at the end of core hydrogen burning. Profiles of poloidal and toroidal magnetic field, angular velocity, and specific angular momentum are shown as functions of the enclosed mass. From https://ui.adsabs.harvard.edu/abs/2005ApJ...626..350H/abstract.

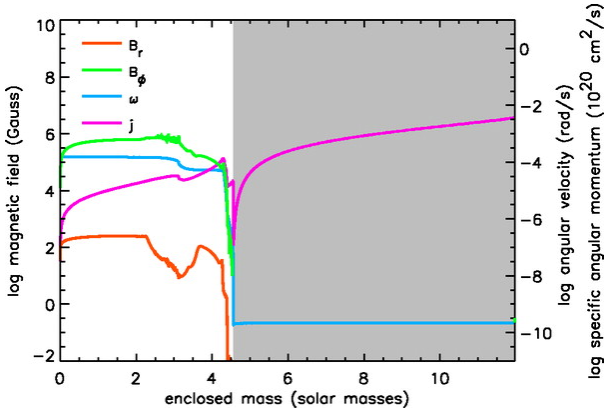

The same, but later in the stellar evolution, at the ignition of central carbon burning. Shaded regions are convectively unstable and, thus, without magnetic field. Compared to the previous figure, the Tayler-Spruit mechanism has redistributed the angular momentum, lowering its value in the centre.

Self-consistent modelling in 3d MHD simulations that can give us detailed information on the processes such as convection and dynamos and thus on the structure of rotation and the magnetic fields has to be restricted to short phases in the stellar evolution. Over the last years such models have been computed for, e.g., convective O burning (https://ui.adsabs.harvard.edu/abs/2021MNRAS.504..636V/abstract) and the O, Ne, C burning shells (https://ui.adsabs.harvard.edu/abs/2023MNRAS.526.5249V/abstract) covering typically a few minutes in the phases immediately prior to core collapse. The simulations show field amplification in the convective regions up to high values and saturation below or at equipartition with the velocity field. A promising avenue of future research consists of feeding the lessons learnt in such 3d models back to the 1d stellar-evolution models in the form of refinement and an improved calibration of the approximate recipes for convection, magnetic amplification, mixing etc.

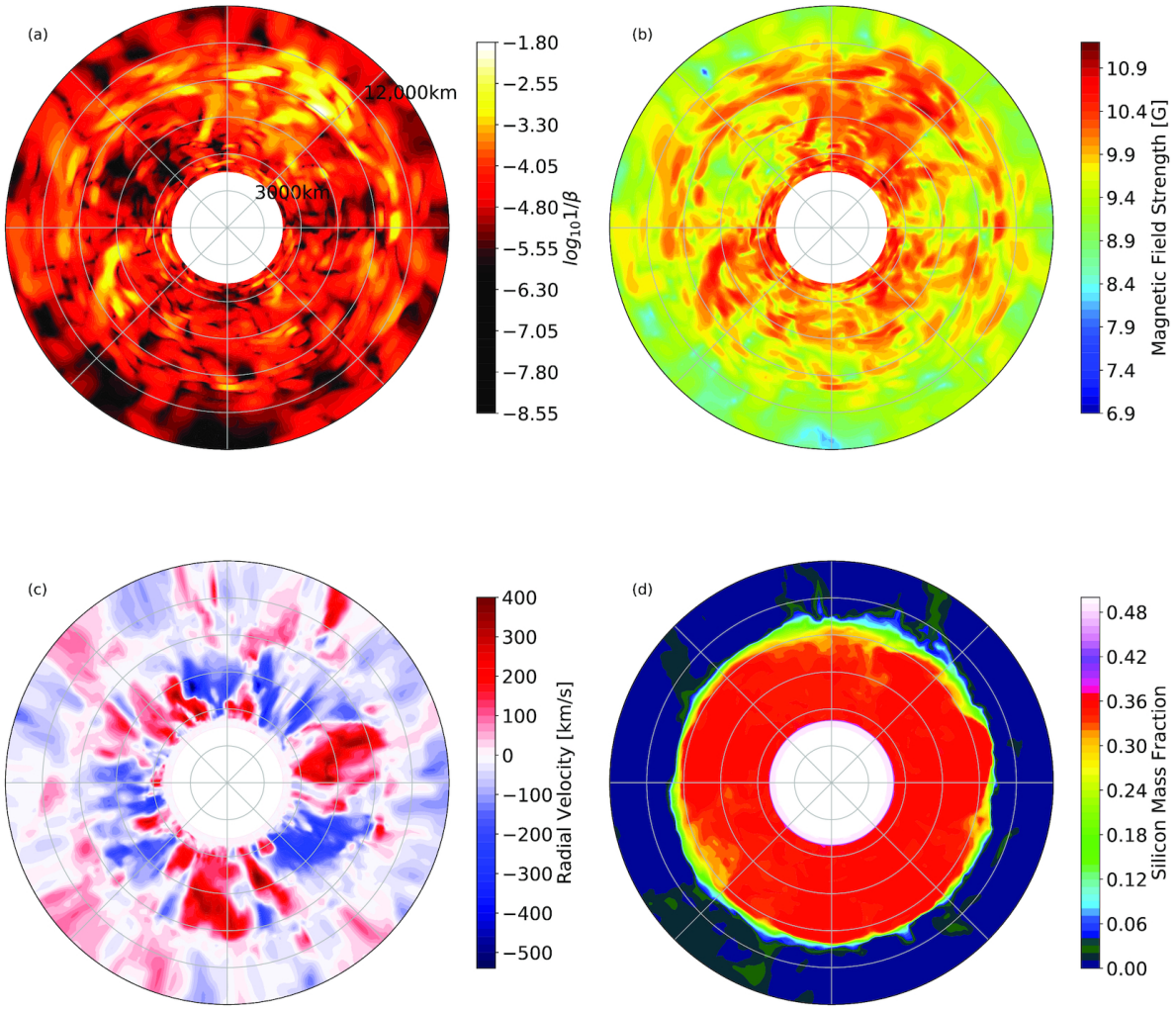

Snapshots of the equatorial plane in a 3d MHD simulation of O shell burning. The panels display (a) the ratio of magnetic-to-thermal pressure (i.e. inverse plasma-β), (b) the magnitude of the magnetic field strength, (c) the radial velocity, and (d) the silicon mass fraction. From https://ui.adsabs.harvard.edu/abs/2021MNRAS.504..636V/abstract.

Binary evolution, very common for massive stars, can have a potentially large impact on rotation and magnetic fields. Mass transfer between companion stars in close orbits can be accompanied by a spin-up of the receptor star. In perhaps the most dramatic consequence of binarity, two stars can merge, a process in which the growth of the magnetic field is almost unavoidable (https://ui.adsabs.harvard.edu/abs/2019Natur.574..211S/abstract). Depending on how much time passes between the merger and the collapse of the merger product, the magnetic field at time of the supernova might be much stronger than in the case of a single-star progenitor. The simulation of Schneider et al. (2019) suggest binary mergers as a way to form SN progenitors with particularly strong magnetic fields.

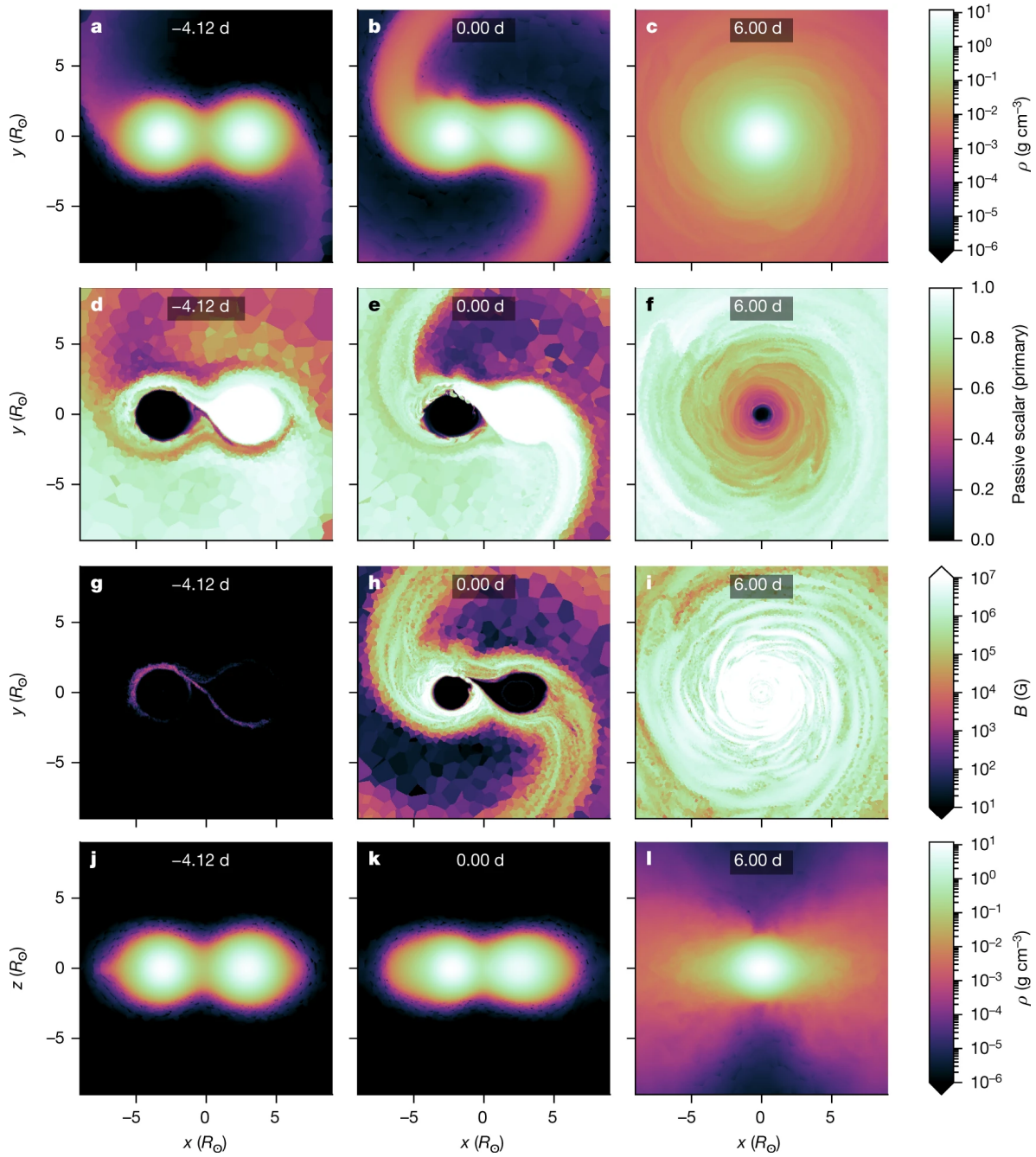

Dynamical evolution of the merger of two main-sequence stars of 9 and 8 solar masses. Panels **a**–**c** show density snapshots in the orbital plane; panels **j**–**l** are edge-on views of the density. The passive scalar (white colour; panels **d**–**f**) indicates material from the 9 *M*⊙ primary and thus visualizes the mixing of the two progenitor stars during the merger. The passive scalar and the magnetic-field strengths (panels **g**–**i**) are shown in the orbital plane. The times given in each panel are relative to the time when the cores of the two stars coalesce (panels **b**, **e**, **h**, and **k**). From Schneider et al. (2019).

https://youtu.be/F8ybsth83VY

Hints on the role of rotation and magnetic fields in CCSNe

Neutron stars: pulsars and magnetars

We have observational information on the rotation and magnetic of the compact remnants of stellar core collapse leads: neutron stars and, to a much lesser degree, black holes. Observations of pulsars reveal rotation rates between milliseconds and a few seconds, which change at rates of $10^{-21\ldots-10}$. If we assume that the loss of angular momentum is due to the presence of a large-scale dipole field, we can convert the loss rate to a field strength (dashed lines) and estimate a typical age of the pulsar (dash-dotted line). The fastest spinning ms-pulsars in the bottom left, which are also the most stable clocks, are likely spun up over millions of years by accretion. Younger objects (the (upper end of the) cloud of black dots) tend to spin slower than those, though still mostly at sub-second periods. Their magnetic fields cluster around $10^{12}\ \mathrm{G}$.

Of particular interest are the magnetars, young neutron stars with very strong fields (two orders of magnitude stronger than the average pulsar) and slow rotation. Further hints for the importance of magnetic fields comes from their electromagnetic emission and occasional flaring activity, which exceeds what can be explained by the loss of rotational energy. Instead, it is thought to be a consequence of the ultrastrong fields.

These observations put constraints on our models of CCSNe. The wide range of parameters hints at the possible existence of several classes of SNe, perhaps corresponding to progenitor classes or stemming from bifurcations during the collapse and explosion phase.

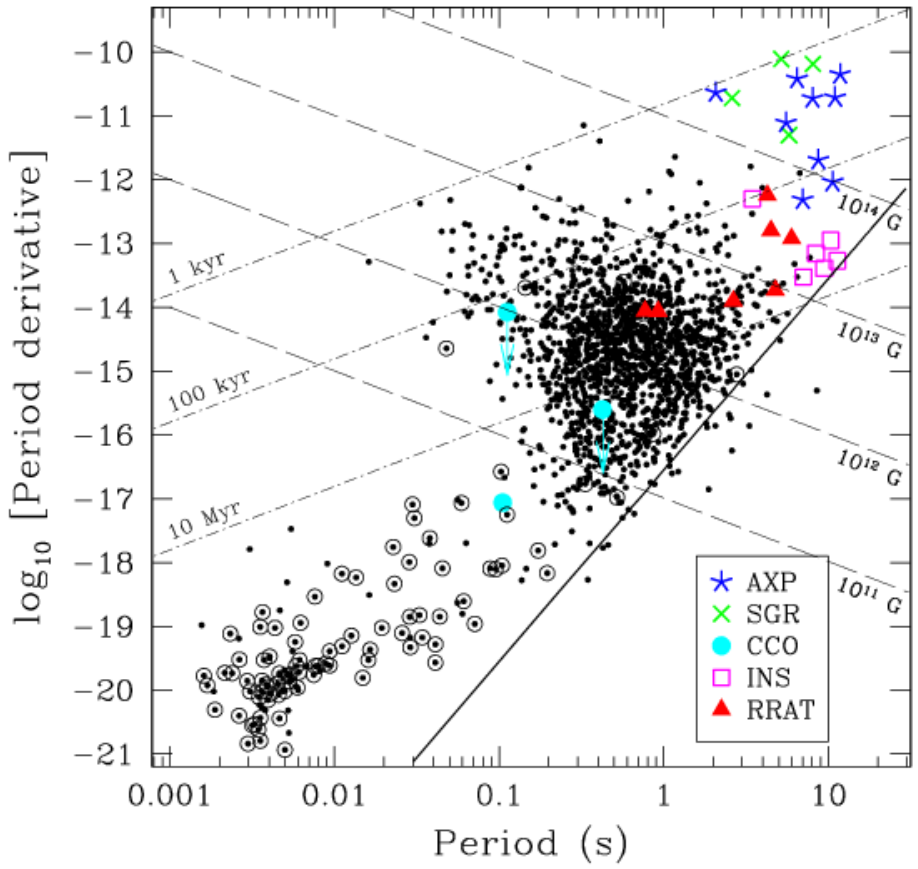

Period and period derivative of neutron stars with several classes indicated by symbols. Kaspi (2010)

Extreme SNe

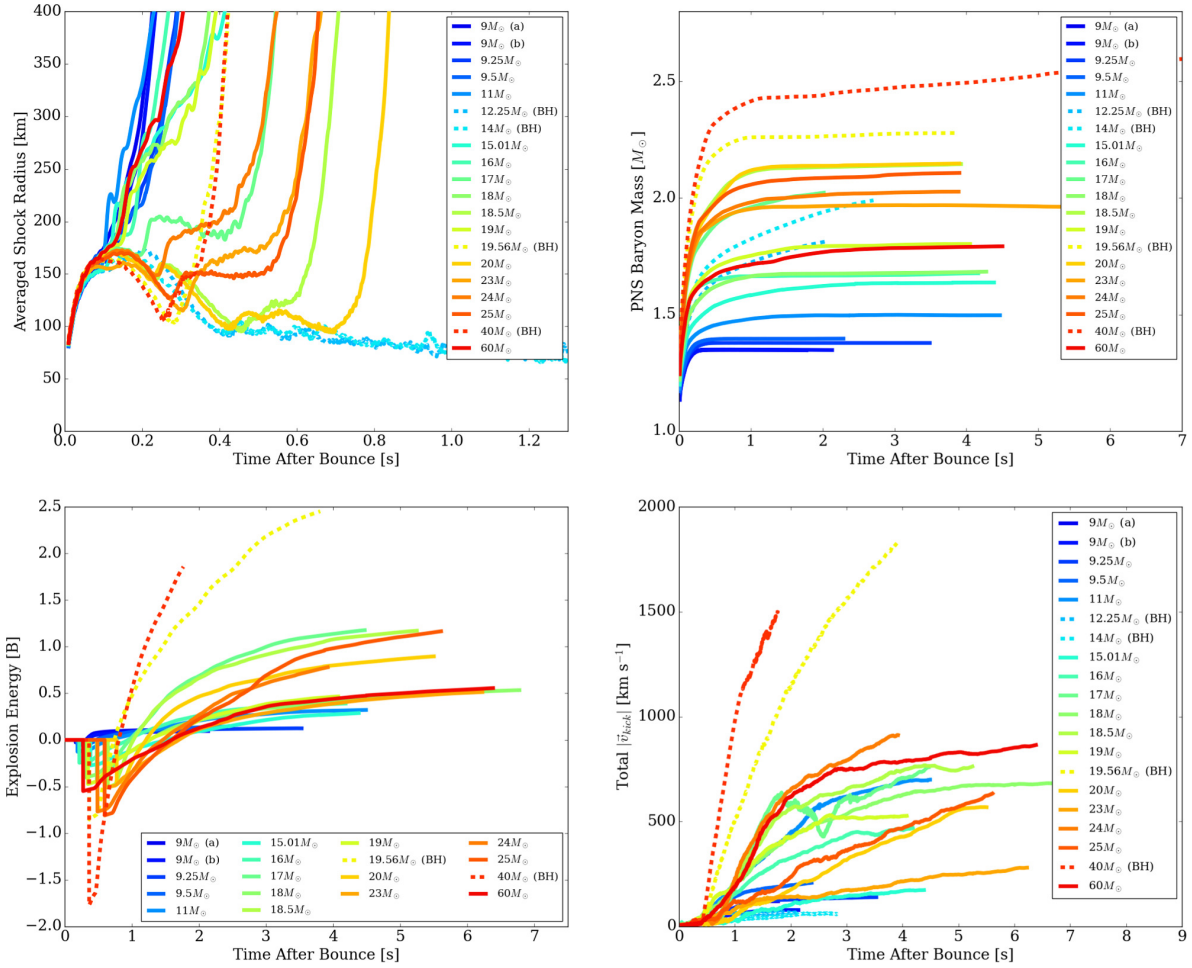

Time evolution of quantities characterising the explosion of 3d models of stellar core collapse without initial rotation and magnetic fields. From Burrows et al. (2024).

Simulations of CCSNe can nowadays be performed with good input physics and in full 3d for several seconds. Keeping in mind that the huge computational costs restrict the number of available simulations and that different groups employing different numerical methods do not always agree on the results for similar stars, and including auxiliary information from additional simulations (e.g., in spherical symmetry and long-term models), a picture tentatively emerges in which the neutrino-driven mechanism successfully revives the stalled shock in many/most cores in the mass range $8...25\ M_\odot$. The properties of the explosion and the compact remnant are compatible with the bulk of the observed populations. The reasonable agreement between models and observations extends to the explosion energies, the masses, kick velocities, spins, electromagnetic emission of the SN, the geometry of the SNRs, the products of explosive nucleosynthesis.

It seems, however, difficult for these models to explain events in the more extreme tails of the observed distributions:

- It seems to be difficult for the neutrino-driven mechanism to achieve the very high kinetic energies observed in hypernovae of several 10^{51} erg and pronouncedly bipolar geometries and

very high outflow velocities likely in SNe associated with GRBs.

- Similarly, some of the most luminous SNe (SLSNe - superluminous SNe) are difficult to explain within the standard mechanism.
- Magnetic fields (and rotation) might deserve a place in an explanation for SNe in which magnetars.
- The possibility of forming the heaviest elements in standard SNe via the r-process is all but excluded based on current models. While neutron-star mergers have emerged as a definite site of the r-process, they need not necessarily be the only one. In particular, the observed early enrichment of galaxies with heavy elements provides hints for an additional r-process channel connected to massive stars.

While the (putative) failure of neutrino-driven in these issues does not unequivocally point to any specific alternative, we will see below that current numerical models support a mechanism involving rotation and magnetic fields as a possible answer to these open questions.

Supernova remnants

The observed SNRs do not provide clear indications either in favour of nor against the role of rotation and magnetic fields in CCSNe. That is partly due to the fact that most objects are observed a long time after the explosion, and in the intervening time many additional effects (e.g., interaction with the environment, hydrodynamic instabilities) might have diluted or even deleted altogether the imprints of the explosion mechanism. There are hints that the youngest SNR observed in great detail, that of SN 1987A, might be the result of a merger progenitor: the axial symmetry of the circum-stellar medium expelled before the explosion suggests so. In other cases, we find pulsar-wind nebulae, in which the young pulsar powers winds and emission via its magnetic spin-down, a process which could be at work also much earlier in the formation of the pulsar.

On a more cautious note, a few of the observed magnetars have been found in an association with SNRs. This class does not differ notably from SNRs hosting ordinary NSs. Thus, the formation of magnetars may not always be accompanied by extreme SNe. This observation could also be interpreted as suggesting to include magnetic fields also in the explanation for ordinary SNe (if one were inclined to give magnetic fields the benefit of the doubt).

The pulsar wind nebula in the Crab SNR. Composite image of optical (red, HST) and X-ray (blue, Chandra).
https://hubblesite.org/contents/news-releases/2002/news-2002-24.html

MHD simulations of CCSNe

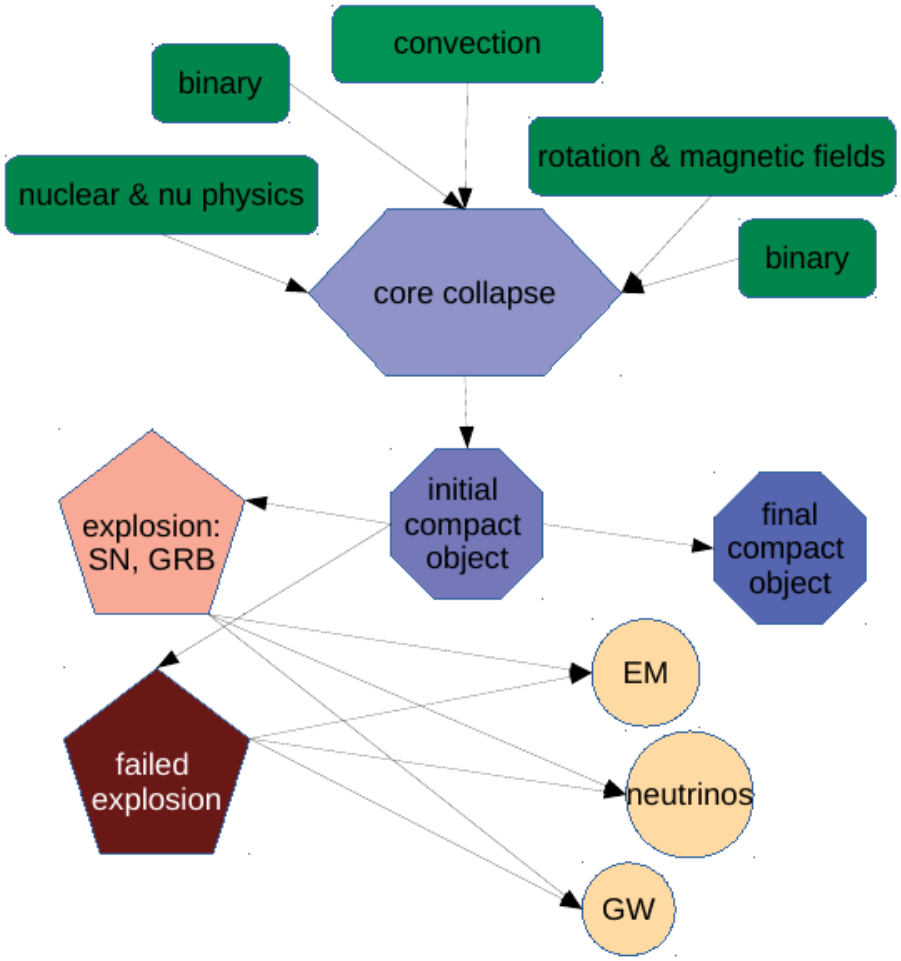

Wish list for the optimal simulation 🎅 and status

- General relativity (and admiral quantum mechanics)
  - Newtonian gravity is not good enough, but approximately GR corrections to the Newtonian potentials yield decent results and are quite common.
- 3d MHD
  - 1d simulations of CCSNe usually only explode if multi-D effects are incorporated via approximate recipes
  - MHD and rotation require at least 2d, but that is also not sufficient as it suppresses important effects (hydrodynamic instabilities, dynamo) or leads to a artefacts
  - 3d is required, but the high computational costs restrict the number of simulations possible; a handful of groups is performing them
    → 1d, 2d simulations are still useful for many questions
- (nuclear) equation of state and nuclear reactions

    - high-density, high-temperature regime: many models in the form of tables from which to chose available
    - choice can have an impact on explosion, PNS, observables
    - sub-nuclear regime: while the EOS is less uncertain, the concrete evolution depends on the nuclear composition. Ideally, get it via the evolution of a large set of isotopes coupled by a nuclear network. Computational costs can be high, though, and often few species with approximate burning are used.
- neutrino physics
    - absolutely indispensable
    - multi-flavour: most commonly $\nu_e, \bar{\nu}_e, \nu_X$, though the full set of six flavours has been used occasionally
    - energy-dependent: as neutrino-matter interaction rates depend on particle energy, grey transport with an assumed (equilibrium, FD) energy spectrum has limited applicability. Though this necessity adds one dimension to the problem, it is standard, albeit with few energy bins only.
    - multi-dimensional transport: mostly used, though in some cases with approximations (ray-by-ray)
    - direct solution of the Boltzmann equation: deemed too expensive in anything but special cases (1d, short simulation times, exploratory studies of specific aspects). Instead, moments methods are commonly used: flux-limited diffusion, two-moment (M1) transport. Their limited description of the angular distribution of neutrinos in phase space causes certain restrictions (artificially interacting rays).
    - velocity (Doppler shift, …) and gravity effects (redshift, …) on the neutrino energies and fluxes are taken into account mostly approximately, sometimes via a full GR treatment
    - neutrino-matter interactions: standard set of reactions includes emission/absorption via beta processes (nuclei, nucleons), scattering off baryons and electrons/positrons, pair annihilation, bremsstrahlung. Differences in implementation and in the inclusion of corrections to the basic reaction rates (weak magnetism, nuclear recoil, magnetic corrections, …) exist.
    - The treatment of flavour oscillations is very much in the beginning. Many analyses of the conditions for various oscillation mechanism in simulations performed without including them explicitly confirmed their potential importance. The inclusion is difficult: short time and length scales over which oscillations occur, explicit dependence on properties of the neutrinos not necessarily available in current transport frameworks. Several groups have attacked the problem from different angles: very detailed studies of neutrino flavours interacting in simplified setups (small boxes) and approximate descriptions in full CCSN models. A lot remains to be done, even very basic work.
- high resolution

    - turbulence has features at scales from many km down to the sub-cm range
    - typical grid resolution of several 100 m in the PNS can be achieved
    - resolving everything is infeasible → convergence studies would be desirable
    - sub-grid scale models for turbulence and unresolved processes
- long simulation times:
    - required to determine the saturation level of explosion energy, composition, ejecta geometry, compact remnant state. Handing off to simulations of later phases, performed with reduced neutrino physics, should be done when the importance of neutrinos on the dynamics is minimal, which takes several seconds.
    - running SN models with full neutrino physics for more than a second is still a challenge
- detailed progenitor models
    - complicated in particular for stars with rotation and magnetic fields by the dearth of multi-dimensional pre-collapse models
    - the explosion dynamics can be quite sensitive to small variations in the progenitor (stars separated by 0.1 Msol in mass may behave surprisingly differently)
- Resources
    - Lots of computing time (typically $\mathcal{O}(1000)$ cores for months): feasible applying for supercomputing time
    - disk space (many TB): can be a headache
    - patience: sometimes a pain somewhere else
- Agreement between groups? Comparing not that simple codes and the results of not all that small simulations is difficult, but would help our understanding of how much of what we see is physics and how much numerics.
- Production of synthetic observables to be compared to observations.
    - With predictions for GW signals and neutrinos as the only direct messengers from the inner engine being standard for simulations, might nature please step up and produce a nearby SN?
    - Electromagnetic signals are produced at a much later stage → comparison requires extending simulations to after shock breakout from the stellar surface.
    - Comparison to NS/BH population and to chemical is similarly indirect and no straightforward

Interlude: state of SN modelling without major role for rotation and magnetic fields

Progenitor modelling

- One-dimensional hydrostatic modelling with codes such as MESA, Kepler, GENEC, FRANEC, PARSEC(, GARSTEC)
  - series of equilibrium models for stellar structure with slow changes of composition, mass,
  - multi-D, hydrodynamic processes such as convection, rotation, magnetic fields are treated with simplified recipes to be calibrated via separate models/theory/observation/experiments: mixing-length, Tayler-Spruit dynamo, ...
  - mass loss (winds, pulsations) and binary mass transfer ditto
  - can follow hundreds of stars from star formation to loss of equilibrium in collapse and reproduce typical HRDs
  - for individual stars, the uncertainties can be considerable, in particular at late phases; example is the debate about the current evolutionary state of Betelgeuse
  - output are radial profiles of density, temperature, composition, ... that can be used as initial conditions for SN models and to assess explosion outcome based on parameters such as the compactness of the core
- multi-dimensional (M)HD models
  - focus on short phases of stellar evolution and perform simulations with (M)HD, nuclear burning, radiation diffusion, neutrino cooling (not transport)
  - for CCSNe relevant topics
    - convective overshoot, mixing, smoothing of shells, shell mergers
    - transport of angular momentum
    - magnetic dynamos
    - stellar mergers
  - feed lessons learned here back into 1d models

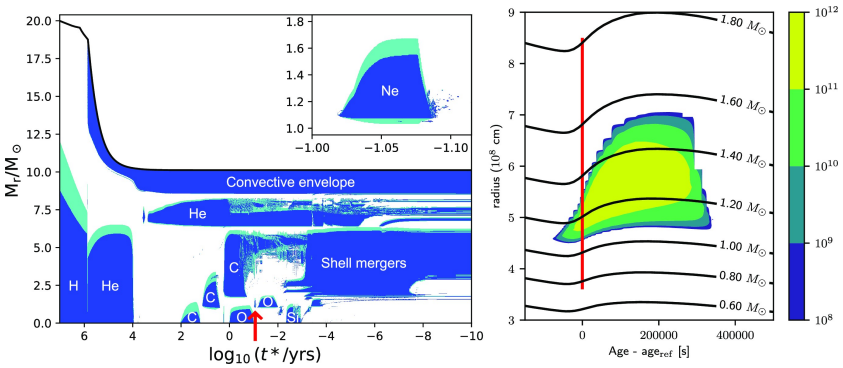

Kippenhahn diagram of a 1d stellar model (20 solar masses, MESA). It shows as a function of time to collapse the location (Lagrangian enclosed mass coordinate) of convective layers (blue) and convective boundary mixing (green). Symbols indicate, e.g., which element is burning. A 3d simulation was launched to study the Ne-burning shell (inset and right) shortly before collapse. From Rizzuti et al. (2023).

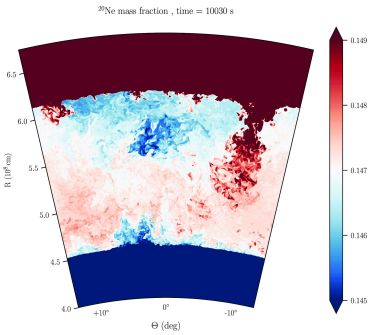

Snapshot of one of the 3d simulation of the Ne burning shell of Rizzuti et al. (2023). Ne-rich material is entrained into the convective layer.

CCSN simulations: (more or less) full physics

- aspirational goal: GR, 3d MHD, 7d neutrino transport with flavour transitions, nuclear reactions, all neutrino-matter interactions, correct nuclear EOS, run for seconds and with high resolution
- we're not there yet and have to live with restrictions due to physical uncertainties and computational limitations
  - pseudo-relativistic potential instead of full GR
  - moments methods for neutrino transport: common approach is the M1 framework in which equations of the type of conservation laws for neutrino energy density and momentum density are solved. The multi-flavour nature is usually taken into account via 3 species ($\nu_e, \bar{\nu}_e, \nu_X$), and the energy dependence is modelled with a modest number of energy bins. M1 methods are mostly good descriptions, but known to develop artefacts (e.g., failing for crossing rays in vacuum).
  - flavour oscillations are still very much at an exploratory stage
  - EOS: phase transitions at high density?
  - computing time is never enough → few models, restricted resolution and simulation time (1 s is considered a long time)
- codes VERTEX, FORNAX, FLASH, CHIMERA, SN3D, Einstein Toolkit, Prometheus-M1/FMT, ALCAR
- Bottom line: while they may not always agree on the detailed evolution of an individual progenitor, **state-of-the-art 3d simulations confirm the viability of the neutrino-driven explosion mechanism**. Explosions develop for many/most progenitors in the mass range $8 \lesssim M_{\mathrm{ZAMS}}/M_\odot \lesssim 25$ with a delay of a few 100 ms. It takes such a time for neutrino heating,

aided by turbulent motions, to revive the shock.

https://prod-files-secure.s3.us-west-2.amazonaws.com/7dc393d7-041f-4dad-abb2-7743053e06ac/877613f9-ec39-4eec-b7fe-1649ad1c4ead/video-Lentz_et_al__2015--3dCCSN.mp4

3d simulation of the neutrino-driven CCSN of a star with 15 solar masses. Lentz et al. (2015)

- The ejecta can be very asymmetric and show a turbulent structure with convective plumes and bubbles of a wide range of sizes.
- It can take a much longer time (seconds) for the explosion energy to reach a saturation level, which is typically of the order of $10^{50-51}\,\mathrm{erg}$, i.e., compatible with typical values derived from observations, including what can be inferred from the neutrinos detected from SN 1987A.
- PNSs are always formed, but they may accrete enough mass to form BH. The compact objects typically gain a non-zero spin and kick due to the random accretion of angular and linear momentum.
- Matters of disagreement are, e.g., which progenitor profiles best predict the success or failure of an explosion, including progenitor asymmetries, the precise landscape of explosions and their energies across the mass range, and in general results for individual stars.

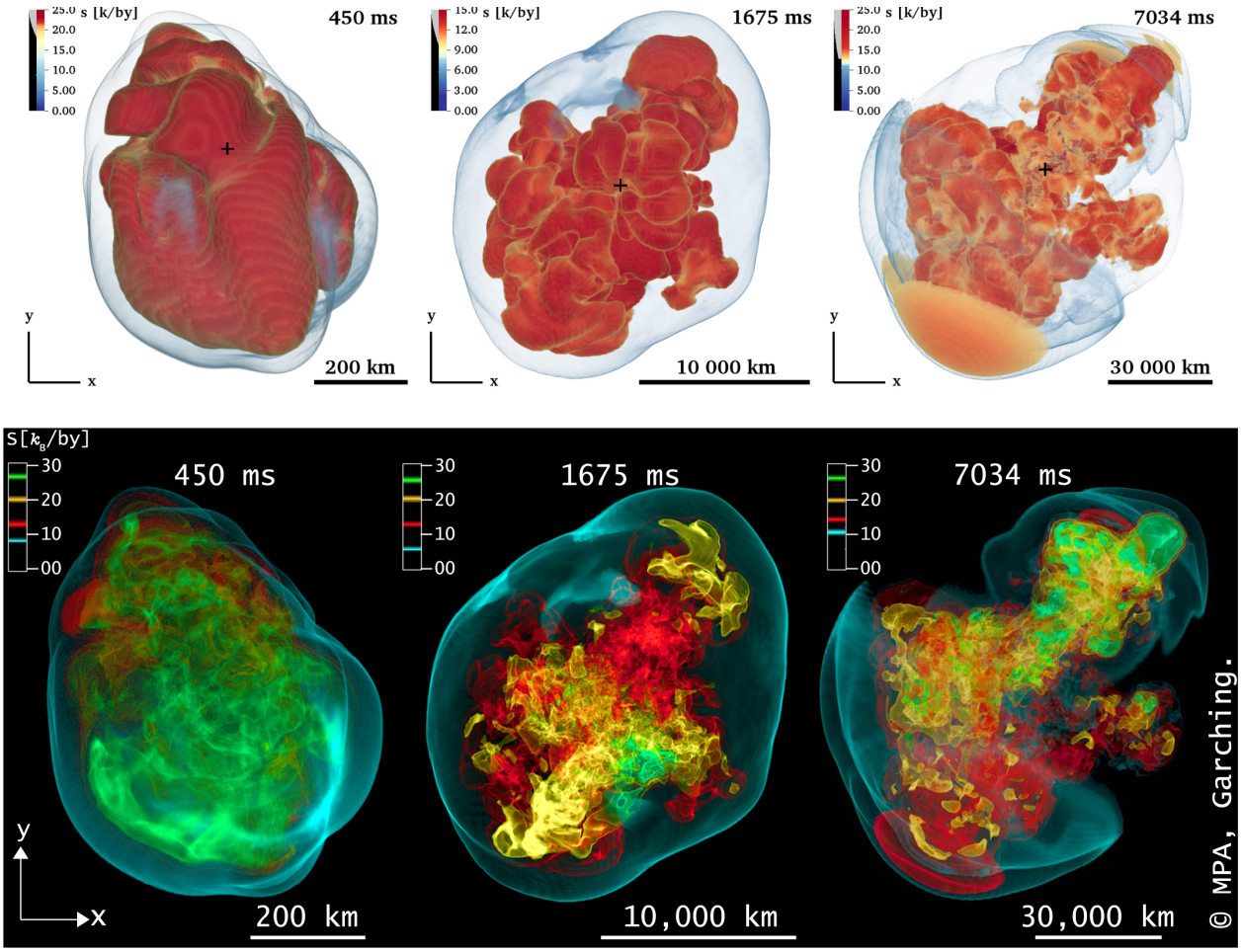

3d model of the neutrino-driven explosion of a star of 18.88 solar masses. Both rows show volume renderings of the specific entropy of the gas at the indicated times. The simulation was run with full and reduced neutrino transport up to and after the 1.675 s (middle panels). The total explosion energy is around 0.2e51 erg, the PNS of 1.8 solar masses, i.e., the compact remnant will be a NS. Model by the Garching group (Bollig et al., 2021).

CCSN simulations: reduced models

- For simulating larger sets, e.g., a fine scan of the mass range, many of the requirements listed above have to be dropped. Simulations employ simplifications such as
  - 1d geometry. Spherically symmetric cores usually do not explode. Hence, an explosion has to be induced artificially by enhanced neutrino heating, a model for turbulence, or simply releasing the energy by hand in the centre or via boundary conditions. Such treatments have parameters that require tuning on simulations in 3d or observations (e.g., to match the explosion energy of SN 1987A).
  - Axisymmetry. Models can explode, though axisymmetry suppresses important flow modes and the properties of 2d and 3d turbulence are quite different and the resulting explosions may not be very true to reality.
  - Reduced neutrino physics, e.g., no dependence on neutrino energy (non-spectral, grey transport) or replacing transport by simplified approaches. That is done quite commonly in

3d models to reach times beyond a few seconds (see below).

- Very useful for exploring which progenitors explode and which fail, what the conditions for nucleosynthesis are, which NS masses or BHs are produced, what the impact of the nuclear EOS on these issues is, for predicting light curves… Large sets of models (fine grids of masses, different metallicities) are necessary for population synthesis or galactic chemical evolution.

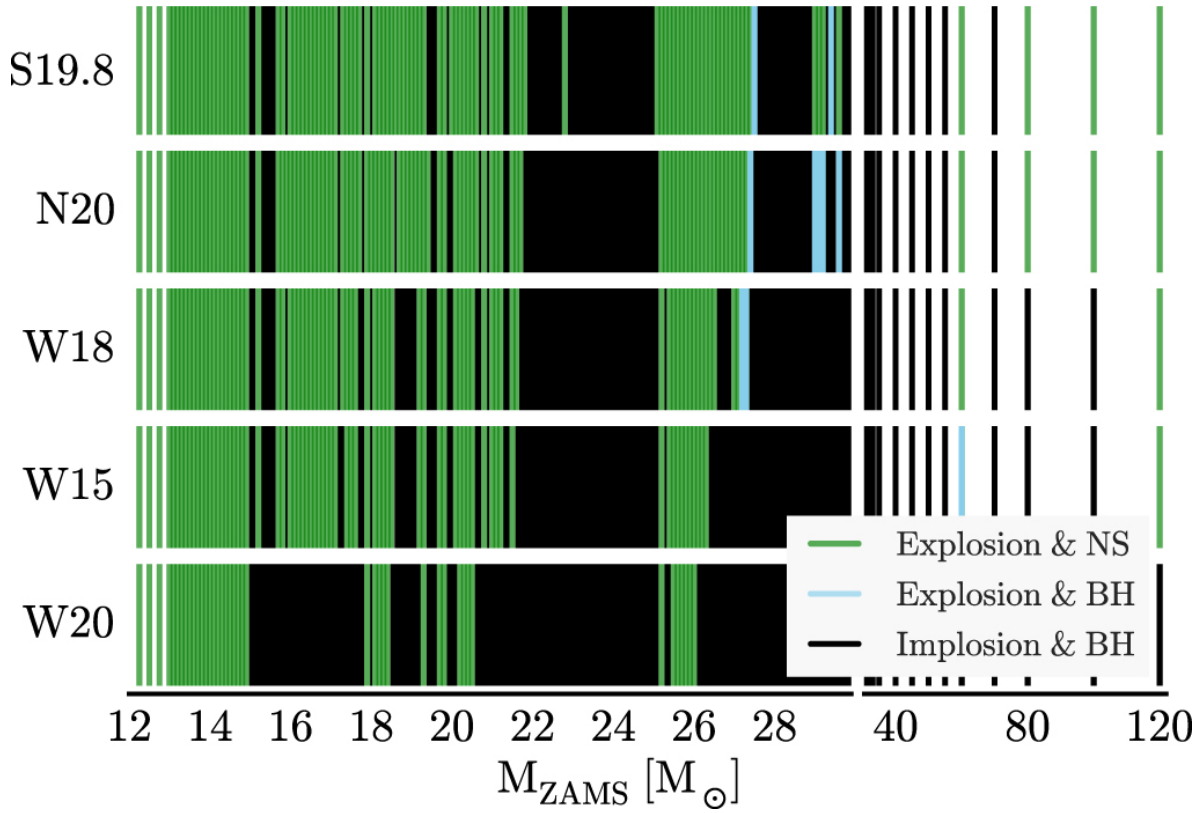

Outcome of collapse in a large number of 1d models with different calibrations (lines). Sukhbold et al. (2016)

Long-term models

- It's a long way from the end of the simulations listed above to the first signal visible in EM bands and the subsequent SN emission and the propagation of the ejecta into the ISM, and it is not a priori clear how, e.g., the early geometry of the ejecta corresponds to that at later phases.
- Methodology to go from a few seconds to thousands of years
  - (gradually) turning off neutrino physics (substituting by less costly methods, then entirely neglecting)
  - ever larger grids with excision of inner part (PNS and NS/BH)
  - potential energy input by central object via inner boundary
  - inclusion of photon transport / photon radiation hydrodynamics
  - energy input of nuclear decays (Ni → Co → Fe, potentially other decay chains)

- partial ionisation
- non-thermal particle acceleration, emission of cosmic rays
- molecule and dust formation
- initial conditions set by the mass loss of the pre-SN star and the surrounding ISM
- synthetic spectra, polarisation in postprocessing using radiative transfer codes

- Growing set of ever more detailed simulations that try to match the better and better observations showing more and more details of the 3d structures

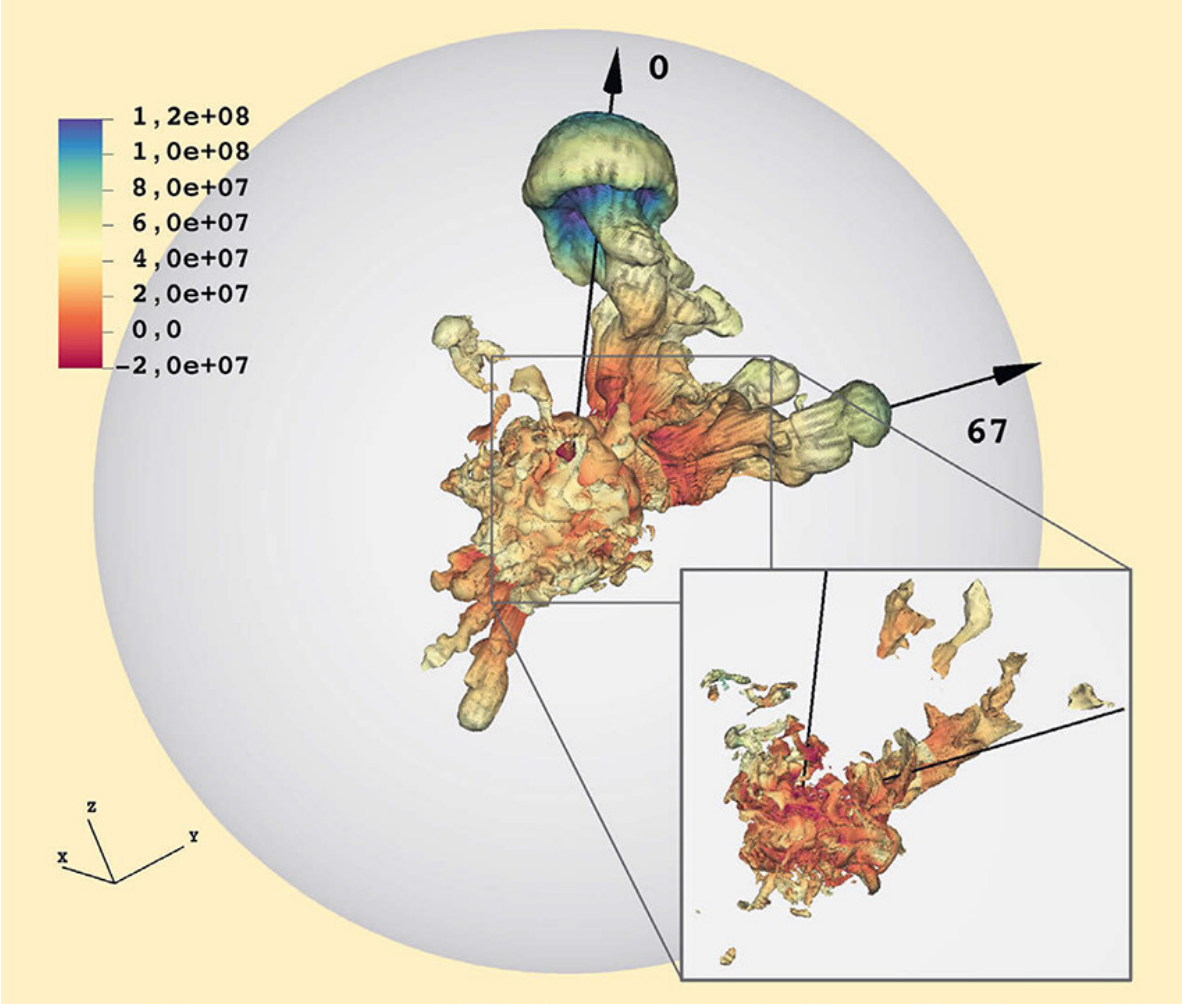

Continuation of a simulation of a neutrino-driven SN at almost 2 days after bounce, shortly before the ejecta reach the surface star (grey). Isosurfaces of 1 % (main) and 10 % (zoom) of Ni abundance are coloured by radial velocity in cm/s. Kozyreva et al. (2022).

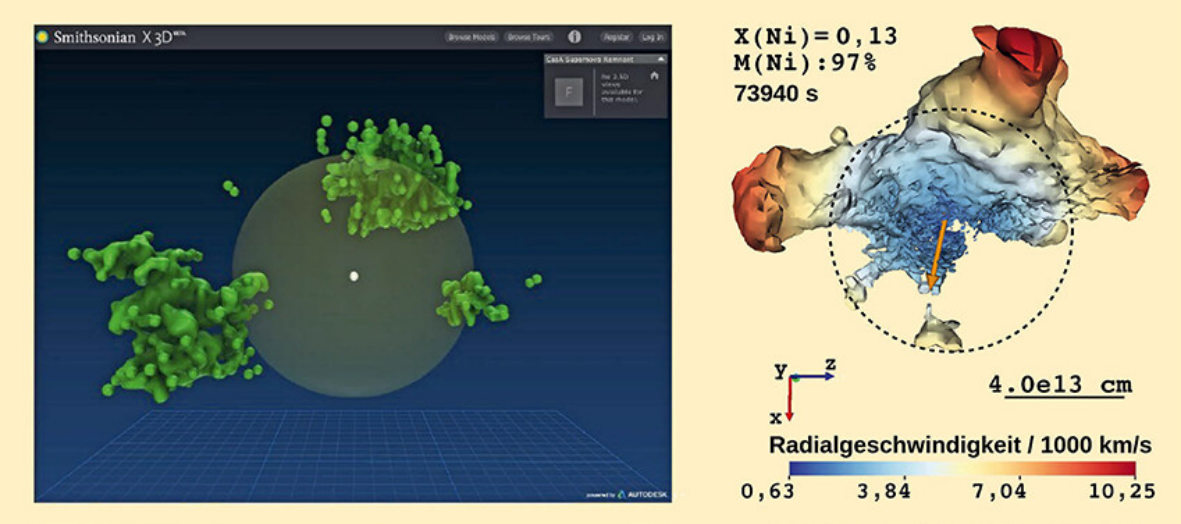

Left: Chandra observations of regions with high Fe concentration in SNR Cas A which shine after being heated by the shock wave indicated via the semi-transparent surface. Right: simulation of a neutrino-driven explosion at a day after the bounce. The surface, coloured in the radial velocity, shows a concentration of 13 % of Ni56 and contains about 97 % of the ejecta mass. Arrow: propagation direction of the NS formed in the explosion. Image taken from Janka (2023), simulation Wongwathanarat et al. (2017).

Status

- neutrino-driven explosions work reliably for many progenitors
- properties of explosions and compact as well as gaseous remnants are compatible with a large fraction of the observed population
- details and some more fundamental questions still await solution
- need for alternative scenarios?
  - explosions driven by (exotic) nuclear physics: phase transitions, axions, sterile neutrinos
  - magnetorotational explosions → extreme events (I very much hope so)
  - jittering jets → no real evidence from simulations

Field amplification processes

The collapse of the core drags the field frozen into the gas with it and, via the compression, amplify the pre-collapse field by 2 to 4 orders of magnitude. Even then, the field does not reach a strength/energy density sufficiently strong to affect the collapse. As the collapse is supersonic, a magnetic field strong enough to change the dynamics would have to be close in energy density to the internal energy, which is not quite achievable given the pre-collapse field.

The angular momentum of a fluid element is conserved very well during collapse as transport processes are slower than the infall. Thus, the angular velocity as well as the rotational energy and the ratio $T/|W|$ of the newly formed PNS are much higher than in the pre-collapse core. Additionally, rotation naturally becomes differential with a gradient $\partial_r \Omega < 0$. Thus, a poloidal pre-

collapse field will be wound up. The amplification proceeds linearly on the time scale of the rotational period, which can be down to the ms regime.

Besides linear winding, the differential rotation can enable the growth of the magneto-rotational instability (MRI). It is based on a positive feedback loop between angular-momentum transport between (initially) nearby fluid elements rotating at slightly different speeds and the amplification of the field via stretching the field lines. If it operates, the field grows exponentially on the time scale of the rotational period, i.e., potentially very rapidly. It leads to the development of MHD turbulence and an efficient outward transport of angular momentum by the field. The energy considerations given above do not apply here: the MRI is a weak-field instability that can work even for (in the idealised situation) infinitesimally weak seed field. There are two main concerns, however:

- Even if the MRI is triggered, whether or not it amplifies the field to dynamically relevant level depends on the amplitude at which the exponential growth saturates, which is an active field of research.
- The MRI grows fastest on length scales that depend on the initial field. The most unstable wavelengths corresponding to typical fields of SN cores can be in the cm range, which is much less than the grid resolution affordable in simulations. Failing to resolve these scales means that the MRI growth is artificially slowed down or suppressed altogether. There is no easy way to overcome the problem, though specialised sub-grid-scale models can be developed.

Most research on the MRI has been done in the context of accretion discs, in which it provides the angular-momentum transport necessary to slow down rotation and allow fluid elements to spiral toward the central object. There, but potentially even more so in stars and CCSNe, it has to be studied together in a background in which other hydrodynamic instabilities may act or a stable stratification may suppress it. Global simulations of the core with full neutrino physics show the growth of the MRI, though the evidence coming from them is limited due to short simulation times and the use of already strong initial fields to deal with the resolution problem.

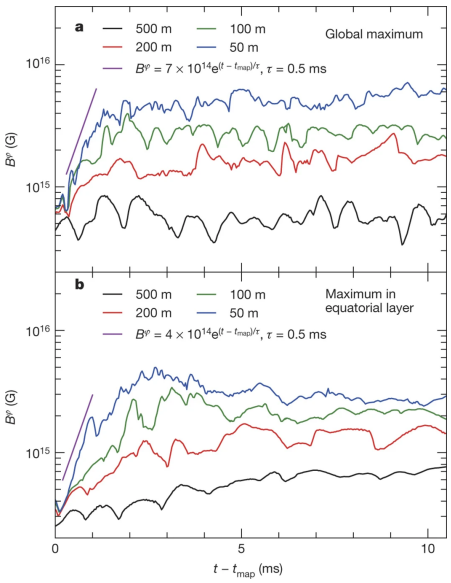

Time evolution of the maximum magnetic field strength in a rapidly rotating PNS in which a large-scale dynamo operates. Different colours indicate resolutions of the simulations. Only sufficiently fine grids can resolve the growth driven by the MRI. Mösta et al. (2015)

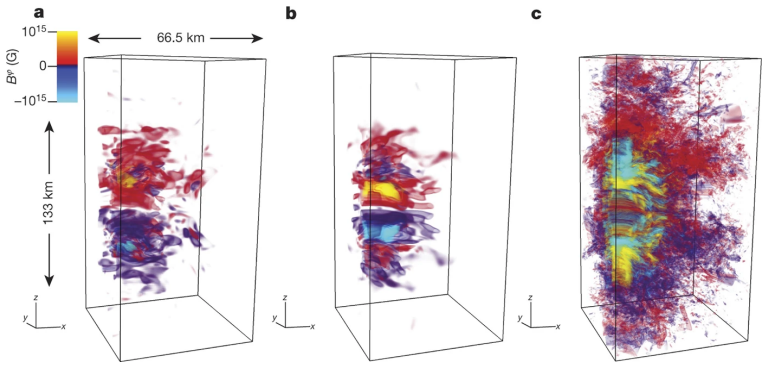

Structure of the toroidal magnetic field in a PNS in which a large-scale dynamo operates and generates strong field with a large-scale north-south asymmetry. Left: initial conditions; middle and right: field at 10 ms for simulations withh 500 and 50 m grid resolution. Mösta et al. (2015)

https://prod-files-secure.s3.us-west-2.amazonaws.com/7dc393d7-041f-4dad-abb2-7743053e06ac/f6f71091-12ea-47b1-8e4a-485a53e82044/aa42368-21-fig4.pdf

Field lines in simplified (anelastic simulation with outer boundary condition and simplified neutrino treatment) PNS model in which a MRI-driven alpha-Omega dynamo after 0.773 s. Colours represent field strength. Reboul-Salze et al. (2022)

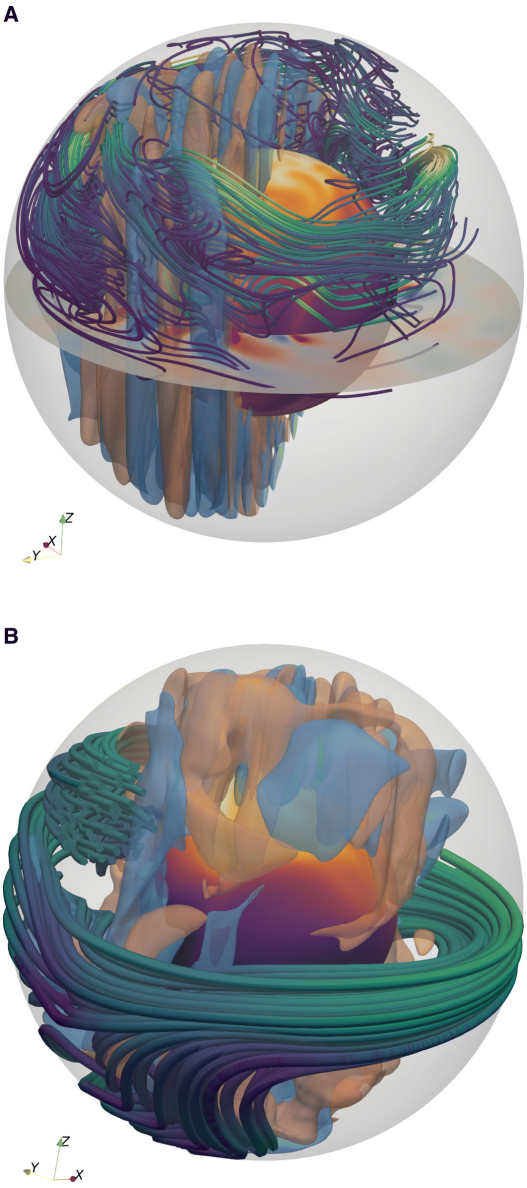

Three-dimensional structure of the field in two different regimes of a convective PNS dynamo. Top and bottom panels show cases in which slower and faster rotation generate weaker and stronger fields, respectively. Magnetar-level fields can be reached via this process. Simulations were possible for long times due to the simplified setup, similar to MRI dynamo above. Raynaud et al. (2020)

Additional channels of field amplification are provided by the hydrodynamic instabilities acting after the core bounce. The standing-accretion-shock instability (SASI) produces turbulence and can

induce a moderate rotation of the PNS. Its role in reviving the shock wave has been questioned, but if it operates, it can amplify the magnetic field around the PNS.

Convection will develop in the PNS as well as in the surrounding hot bubble behind the shock wave. A turbulent dynamo is a very plausible consequence. If rapid rotation, compared to the overturn time scale of convective eddies, is present, a large-scale dynamo can develop and with it a large-scale dipole field; otherwise, strong a field strength is also possible, though it would be limited to smaller scales. Conditions for the both cases can be investigated even without running simulations with an actual magnetic field. White et al. (2022) evaluated them based on 3d models and inferred that a convective dynamo can naturally lead to the fields observed in pulsars and magnetars. Of course, simulations with magnetic fields are needed to settle the question. Raynaud et al. (2020) performed a series of simulations of convective dynamos in simplified models for PNSs, in which the global dynamics was excluded and neutrinos were treated in an approximate way. They confirm the existence of the large-scale and small-scale regimes of dynamo action and find saturation fields up to the magnetar level. Simulations with full neutrino-MHD are desirable to advance on this issue. Furthermore, in convectively stable regimes, the Tayler-Spruit dynamo, as proposed for pre-collapse stars, can operate, as shown by by Barrère et al. (2023).

https://prod-files-secure.s3.us-west-2.amazonaws.com/7dc393d7-041f-4dad-abb2-7743053e06ac/440d18a5-1de4-48ae-b7fa-66a21212e272/Blondin_Mezzacappa__2010__S3.webm

SASI-unstable core: Blondin & Mezzacappa (2007)

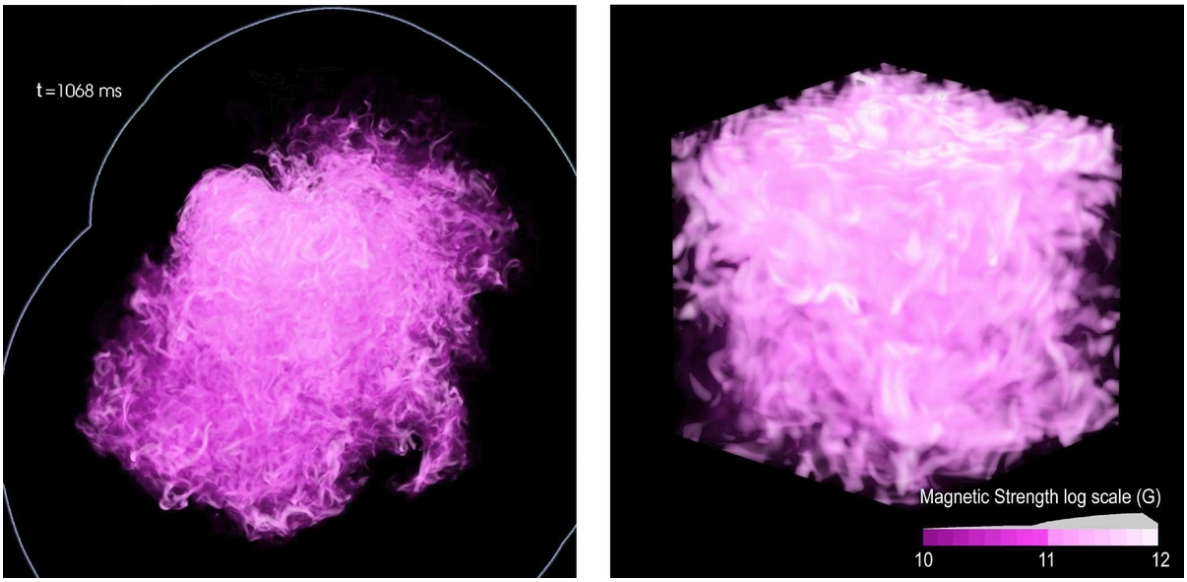

Structure of the magnetic field in a core in which the spiral mode of the SASI operates at about 1 s after bounce. The right panel is a zoom into the larger left panel. The turbulent motions of the flow have generated a strong field (nearing equipartition with the kinetic energy) with compex structure. Endeve et al. (2012)

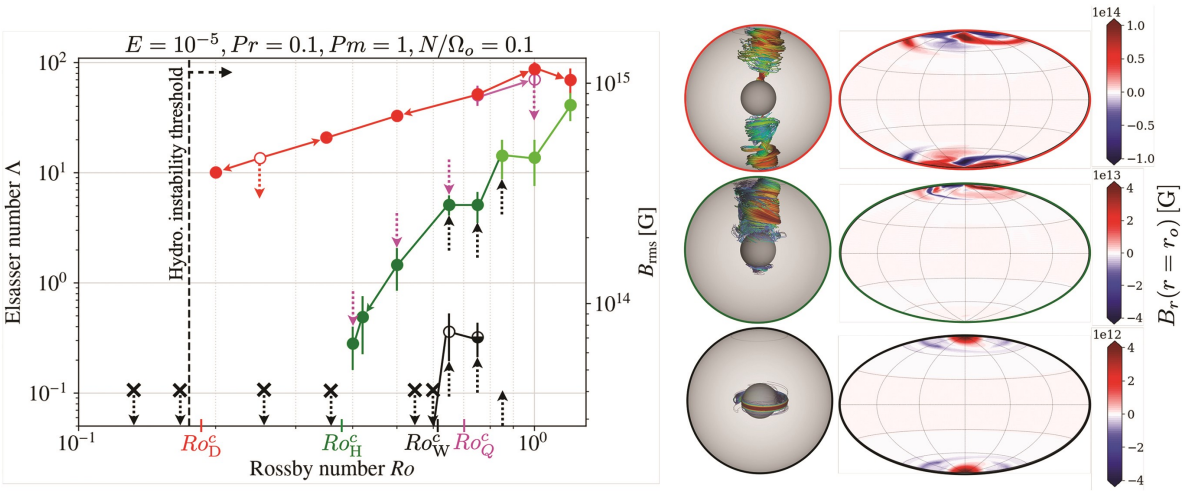

Different regimes of the Tayler-Spruit dynamo in a convectively stable PNS. The right panel shows the possible field structure, which includes solutions with bipolar and unipolar large-scale fields and weaker fields. Again, a reduced simulation setup as above. Barrère et al. (2023)

Dynamics

If and when magnetic fields (locally) grow to sufficient strength, they can affect the dynamics in various ways:

1. They can change the evolution of convective regions, e.g., by stabilising smaller eddies, which and favouring the development of larger ones. The consequence can be an easier shock revival in magnetised cores.

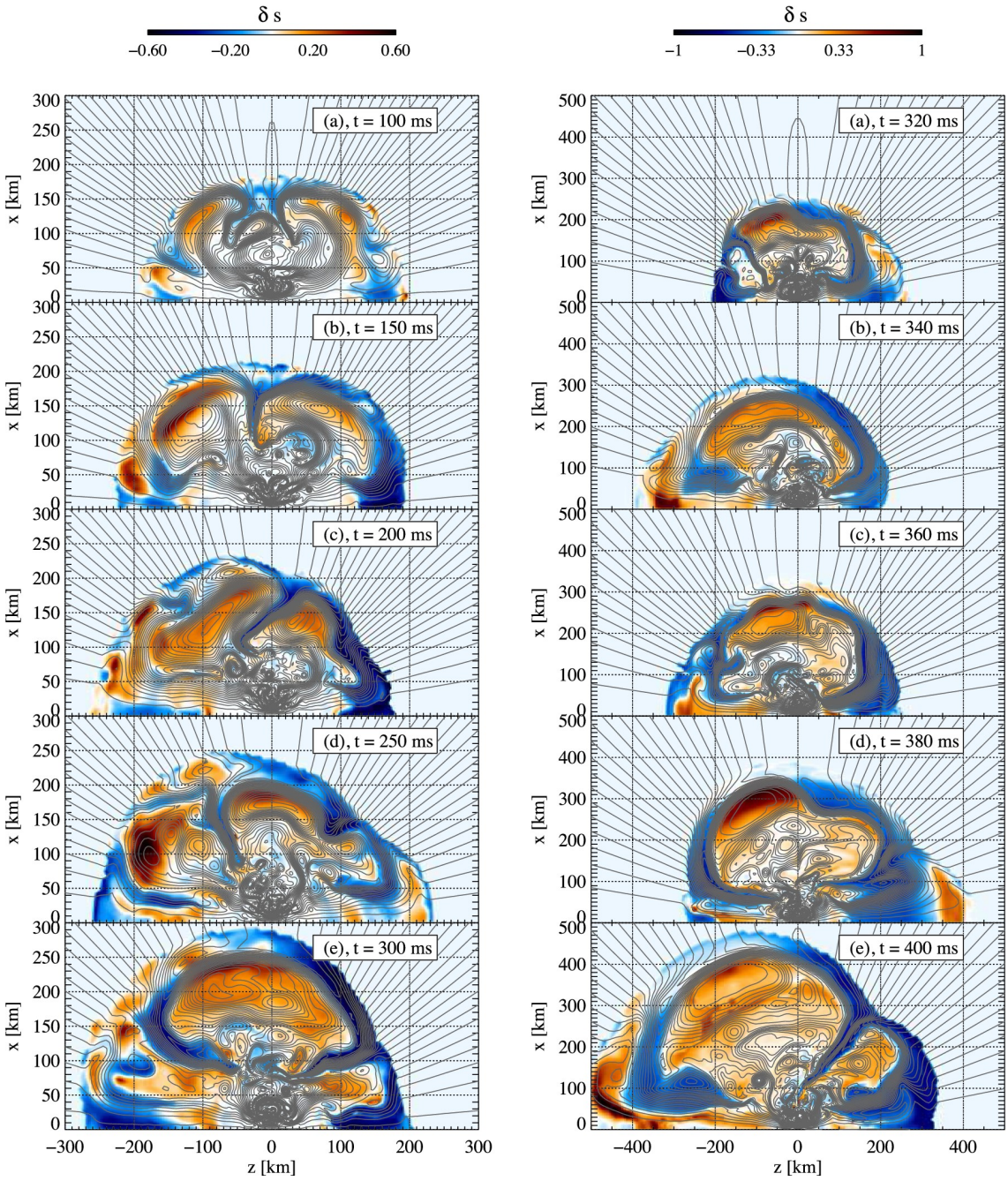

Time sequences of entropy (deviation from angular average) and magnetic field lines in axisymmetric models of core collapse without rotation, but non-zero magnetic field. Large-scale convective bubbles form. They are shielded by the field lines, which give them more stablity. Obergaulinger et al. (2014)

https://prod-files-secure.s3.us-west-2.amazonaws.com/7dc393d7-041f-4dad-abb2-7743053e06ac/b9fb546b-36a2-459a-ab92-856f5e44a533/Magnetised_SN_2d_simulation--entropy.webm

2. MHD turbulence behind the shock wave can, just like non-magnetic turbulence enhance the effectiveness of neutrino heating and thus favour shock revival.
3. The transport of angular momentum from a rapidly rotating PNS to the surrounding layers allows for the extraction of rotational energy and can aid or even fully power an explosion. This dynamics can play out in several scenarios:
    a. A small-scale turbulent field, e.g., generated by the MRI, can act as an effective viscosity transporting angular momentum gradually outward. The PNS can consequently lose rotational support and contract.
    b. Large-scale fields can operate in a version of the pulsar spin-down mechanism. They can launch magnetised winds from the PNS surface or the layers surrounding it. This mechanism is not limited to the first seconds after core bounce, but can work even after the explosion has started, in a continuous transition to the phenomenology of pulsar-wind nebulae. Depending on the available rotational energy and the field strength, a large variety of phenomena can be driven by PNS/proto-magnetar winds, including various classes of GRBs (Metzger et al., 2011).

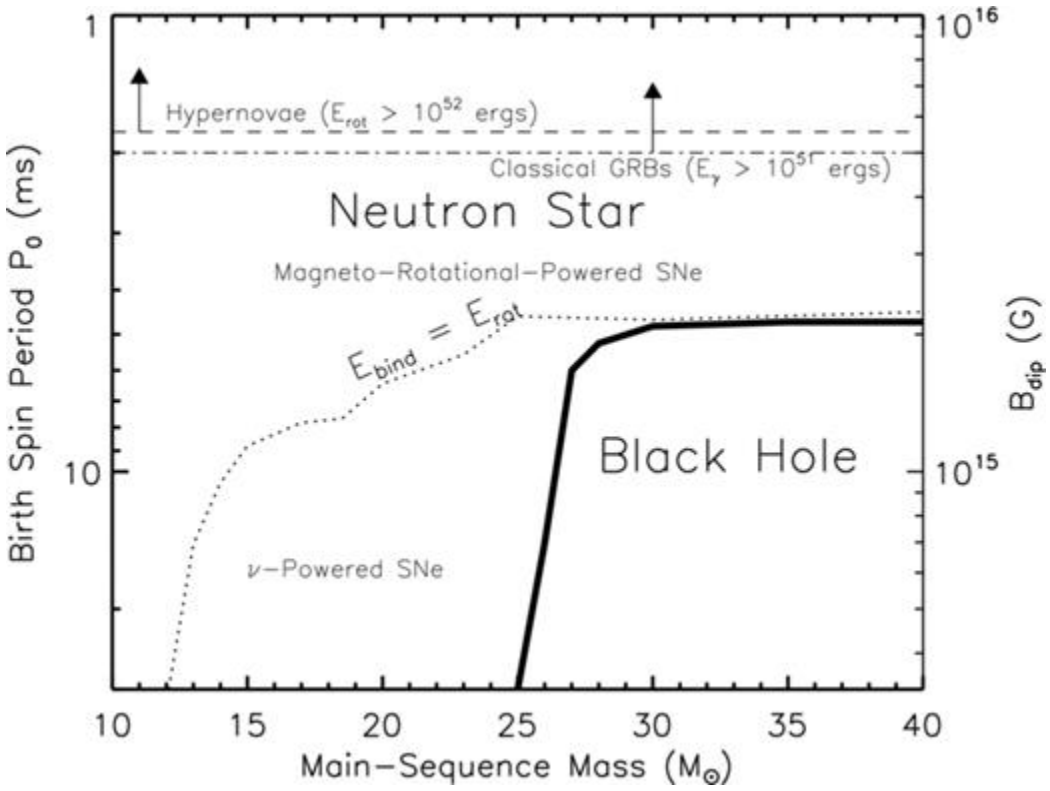

Schematic diagram of the regimes of NS versus BH formation in core-collapse SNe at subsolar metallicities (solid line) in the space of the main-sequence mass and initial proto-NS spin period *P*0, taking into account the possible effects of rapid rotation and strong magnetic fields. The dotted line denotes the rotation rate above which the NS rotational energy *E*rot exceeds the gravitational binding energy of the progenitor envelope. The dashed line denotes the rotational energy *E*rot = 1e52 erg sufficient to power a 'hypernova'. The right-hand axis shows the magnetic field strength, *B*dip, that would be generated if the magnetic energy in the dipole field is ~0.1 per cent of *E*rot. The dot–dashed line is the minimum rotation rate required for a magnetar with a field strength *B*dip to produce a classical GRB with energy *E*γ > 1e50 erg. Metzger et al. (2011)

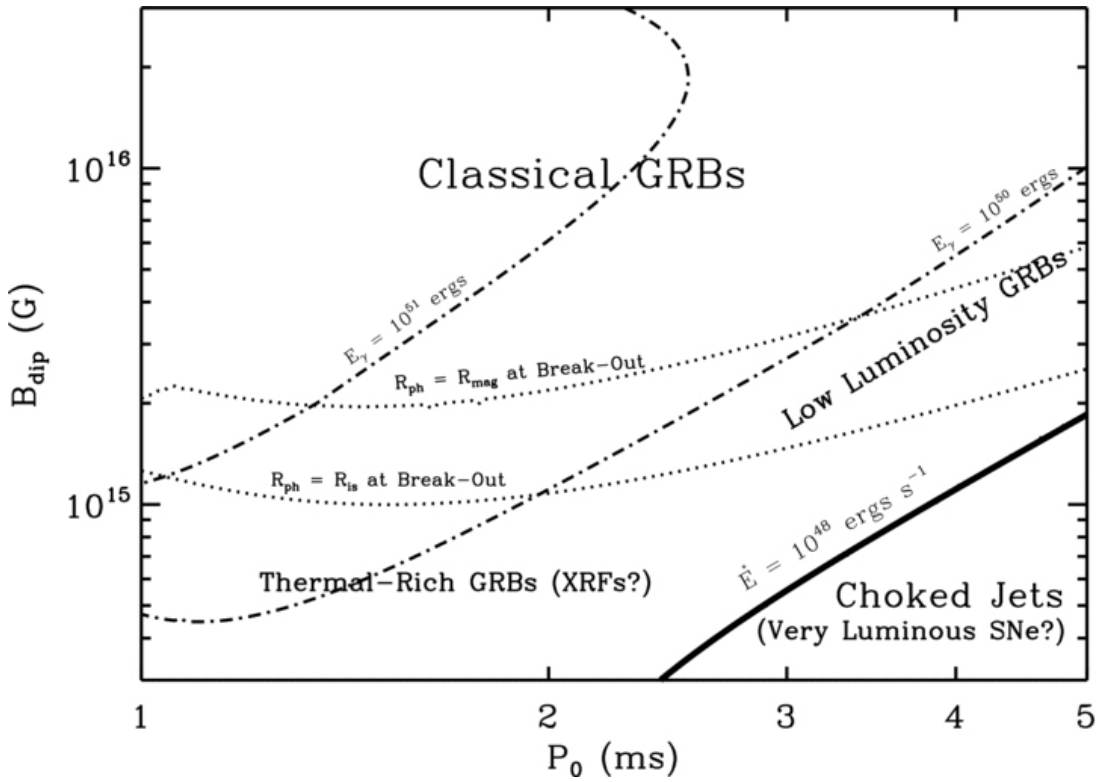

Regimes of high-energy phenomena produced by magnetar birth in core-collapse SNe, as a function of the magnetic dipole field strength, *B*dip, and initial rotation period, *P*0, calculated for an aligned rotator (χ = 0). Metzger et al. (2011)

4. In the presence of large-scale fields, the ejecta are often directed along the rotational axis and collimated into jets. In the case of CCSNe, at least early on, the gas in the jets has high, though not highly relativistic speeds and forms a relatively wide opening angle. As the explosion proceeds, the jets can become faster and more collimated. The jet acceleration is often driven by regions of high magnetic pressure next to the polar caps of the PNS where the field lines form a magnetic tower that expands rapidly in the axial direction. Collimation is provided by the surrounding stellar material in which rotation forms a low-density funnel around the axis.
   It is not guaranteed that jets maintain their collimation and high speeds up to the stellar surface. If the energy input at the jet base ceases, they can be choked inside the star and transform into wide outflows of slower velocities. Furthermore, magnetised jets can suffer from various genuinely non-axisymmetric instabilities such as kink modes that would distort and slow them down or even disrupt them entirely. Whether this actually happens, depends on several factors such as the field geometry of the jet or its speed. Simulations have shown both stable and failing jets.

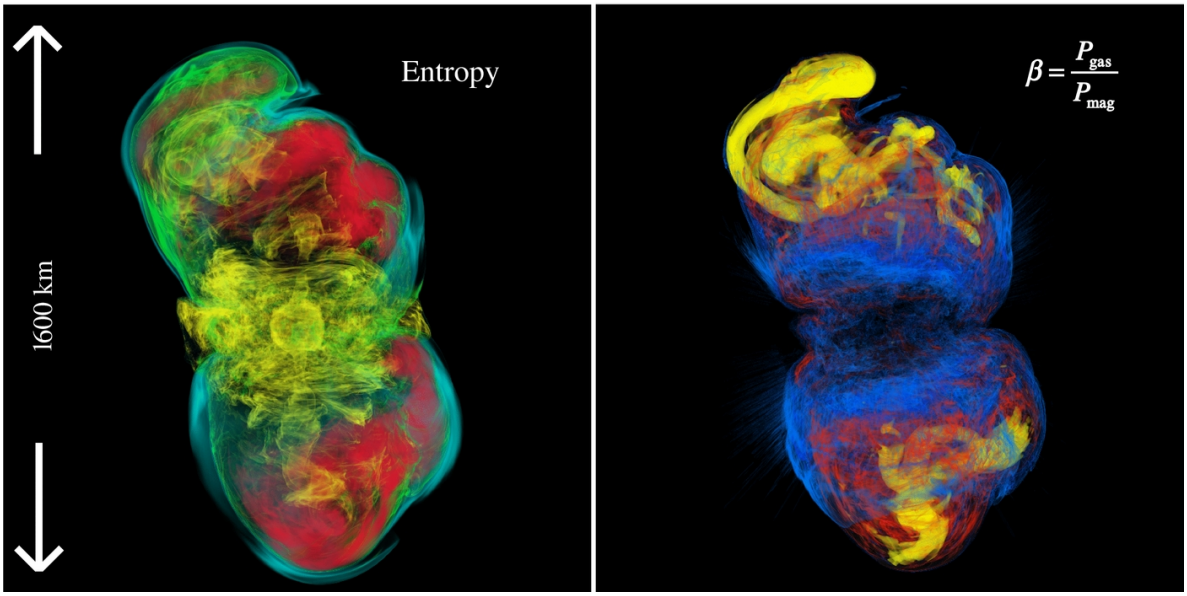

A MHD jets develops in a 3d magnetorotational core collapse, but is disrupted by a rapidly growing instablity. Left: volume rendering of the specific entropy of the gas. Right: rendering of plasma beta. Mösta et al. (2014)

https://youtu.be/3sZmvbtli1I

https://youtu.be/sQQnlHFaVx0

https://youtu.be/hJAY22ZjBMY

Videos of the simulations of Mösta et al. (2014): comparison between axisymmetric and 3d simulation.

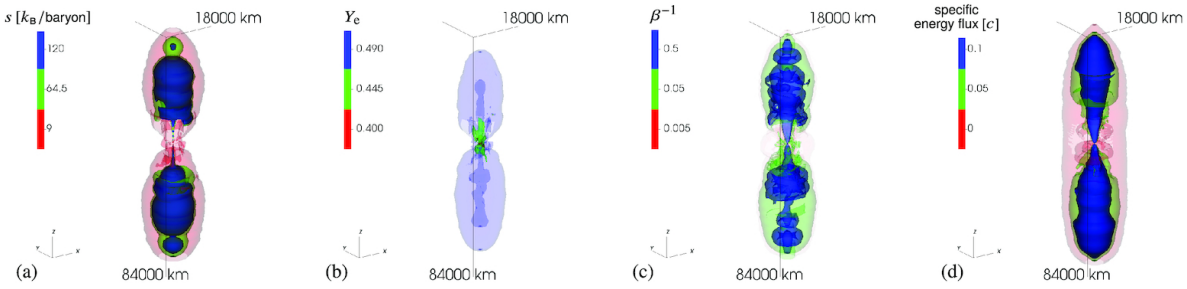

Four variables characterising a jet in a magnetorotational SN model that is not disrupted by instabilities: specfic entropy, electron fraction, inverse plasma beta, specific energy flux. Obergaulinger & Aloy (2021)

https://prod-files-secure.s3.us-west-2.amazonaws.com/7dc393d7-041f-4dad-abb2-7743053e06ac/73256785-17fd-460b-b5ae-5ea7366d3a67/A17-Entropy-contours.webm

Isosurfaces of specific entropy of an explosion on the spectrum between the neutrino-driven and the magnetorotational mechanism. Progenitor mass is 17 solar masses.

https://prod-files-secure.s3.us-west-2.amazonaws.com/7dc393d7-041f-4dad-abb2-7743053e06ac/1a4f4c05-1604-4222-b4c1-0dc2fca1970a/A13-Entropy-contours.webm

Isosurfaces of specific entropy, 13 solar mass star.

https://prod-files-secure.s3.us-west-2.amazonaws.com/7dc393d7-041f-4dad-abb2-7743053e06ac/0c54ab40-f5bc-4b77-9b01-1869a5dcc705/A13-Yn-contours.webm

Isosurfaces of neutron fraction, same core.

https://prod-files-secure.s3.us-west-2.amazonaws.com/7dc393d7-041f-4dad-abb2-7743053e06ac/ed77cb93-6d75-4f03-a3ea-2ad5a7f4aab0/A39-Entropy-contours.webm

Magnetorotational explosion, followed by BH formation for a 39 solar mass star.

Observables and nucleosynthesis

For nearby (i.e., galactic) events, the imprint of rotation and magnetic fields could be observed in the neutrino and GW signal.

1. The PNS rotation might be reflected in a periodic modulation of the neutrino emission, analogously to the lighthouse effect responsible for the periodicity of pulsars. Detecting this kind of signal would require a high count rate and fast detector response. Walk et al. (2018) explored the possibility of employing neutrinos as gyroscopes to detect the rotation of the core.
2. The ringdown of a newly formed PNS with non-zero rotation proceeds aspherically, which gives rise to a characteristic GW signal at bounce. It lasts for a few ms and could be used to infer the rotational energy, potentially even distinguish between EOSs. Furthermore, rotating stars may also produce stronger GW emission than non-rotating ones in the long run, after the bounce has taken place.

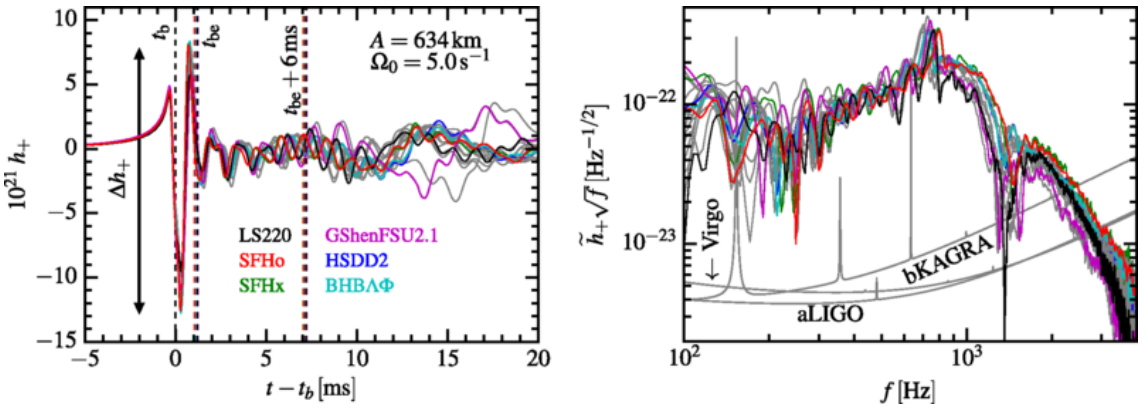

The bounce signal of a rotating core collapse in axisymmetry for different EOSs and roation rates (left) and its Fourier spectrum (right). Richers et al. (2017)

3. As rotation modifies the oscillation modes an a PNS, thus changing the associated GW signal coming from, e.g., the g-modes behind some of the most characteristic signals coming from CCSNe. A systematic investigation of the differences in PNS oscillations between rotating and non-rotating PNSs is required for a better understanding.
4. If a jet is produced, the very asymmetric flow leads to the emission of a very strong GW amplitude. However, its frequency is too low to be easily detectable in the currently operating LVK detectors. Future observatories (ET, CE, DECIGO) might be able to discover such signals.

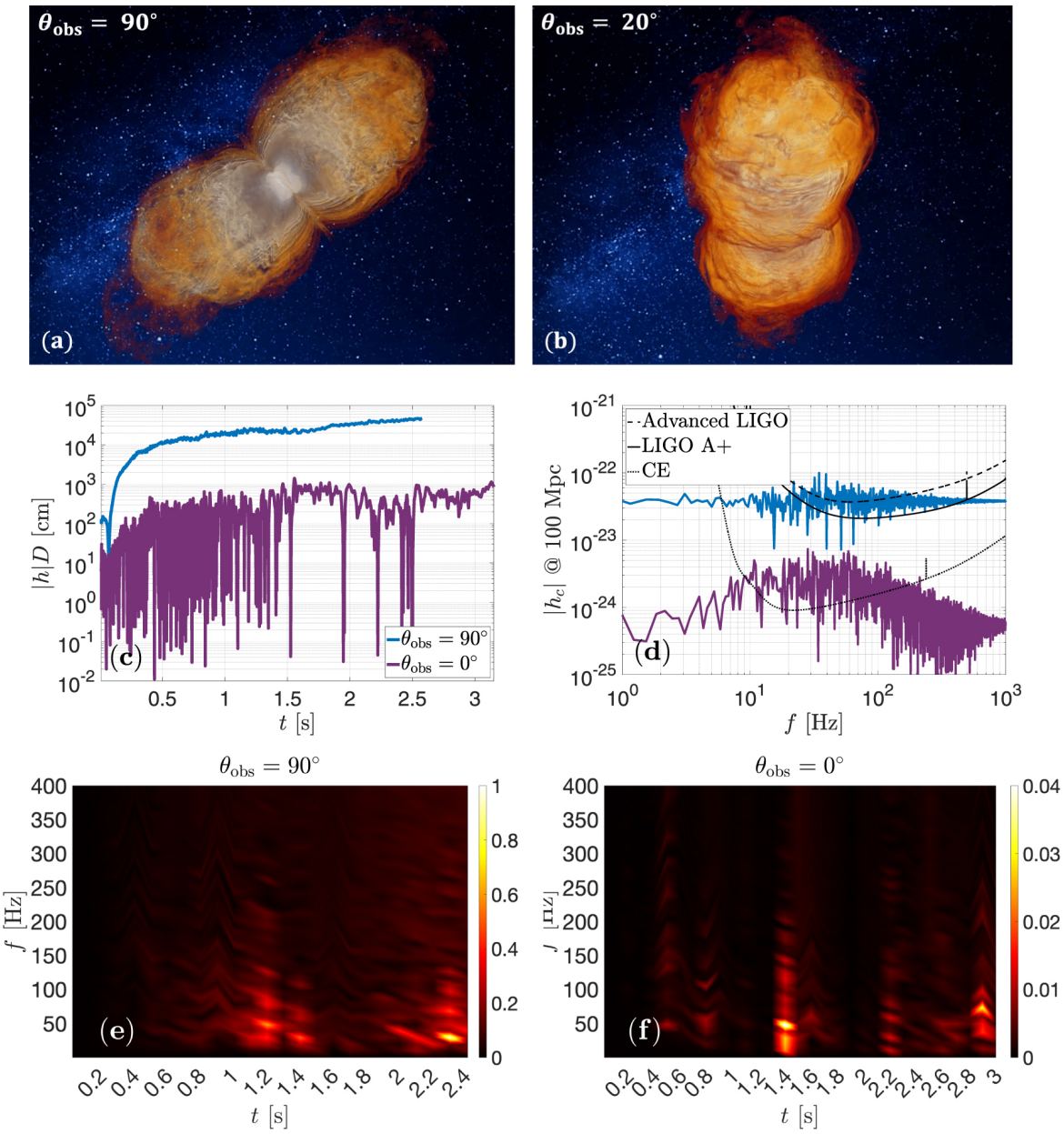

Structure of jets in collapsar GRBs, their GW signal as observed from different orientations in time and frequency domain, and spectrograms. Long-term relativistic simulations, Gottlieb et al. (2023)

The electromagnetic emission of SNe can bear the imprint of rotation and magnetic fields via:

1. The formation of heavier elements than usual. Being less dependent on neutrino heating for the unbinding and acceleration of the gas, these events can reach lower electron fractions in the ejecta. If conditions are sufficient for a (partial) r-process, the synthesised isotopes might reveal themselves in the SN spectra.

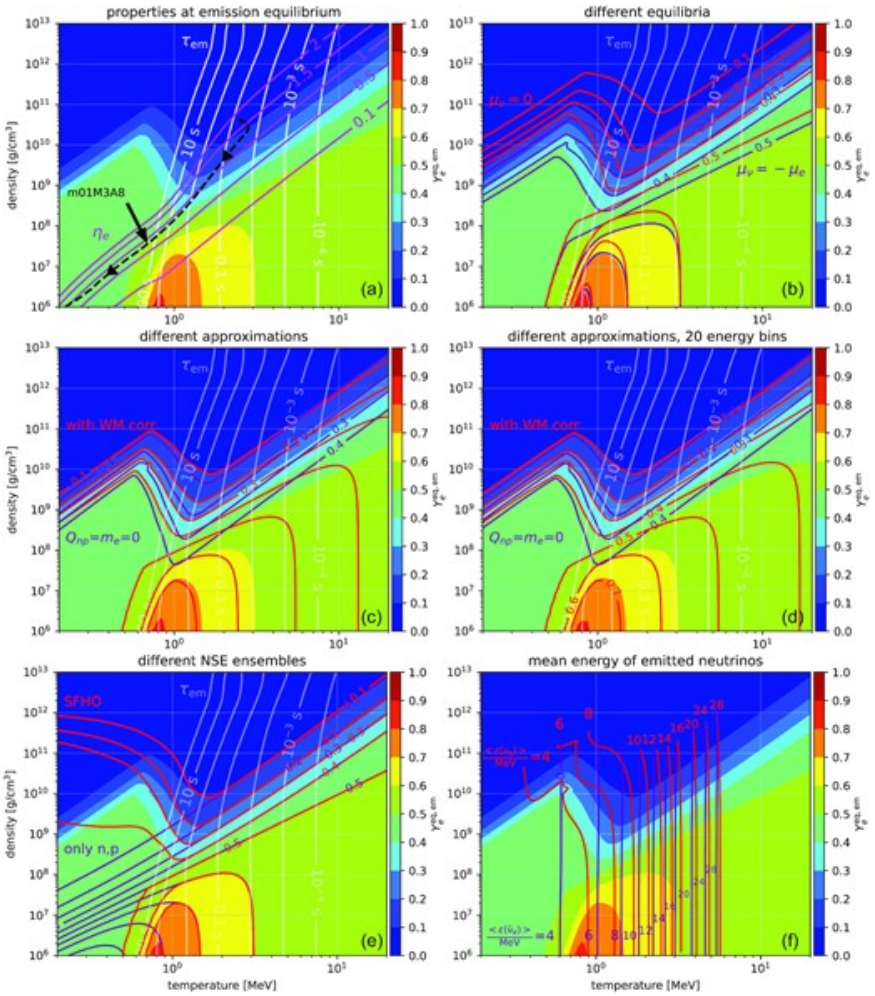

Equilibrium electron fraction for conditions in SN cores or post-merger discs. Neutrino absorption leads to relatively high values, which are detrimental to r-process nucleosynthesis. Just et al. (2022)

2. Energetic SNe driven by jets can produce more Ni than standard events. The result would be a higher luminosity over times of months.
3. The energy injected by a magnetar spinning down will heat the expanding SN ejecta and enhance the luminosity. Magnetars have been invoked as explanation for the majority of superluminous SNe produced by from stripped-envelope stars (type-I SLSNe).

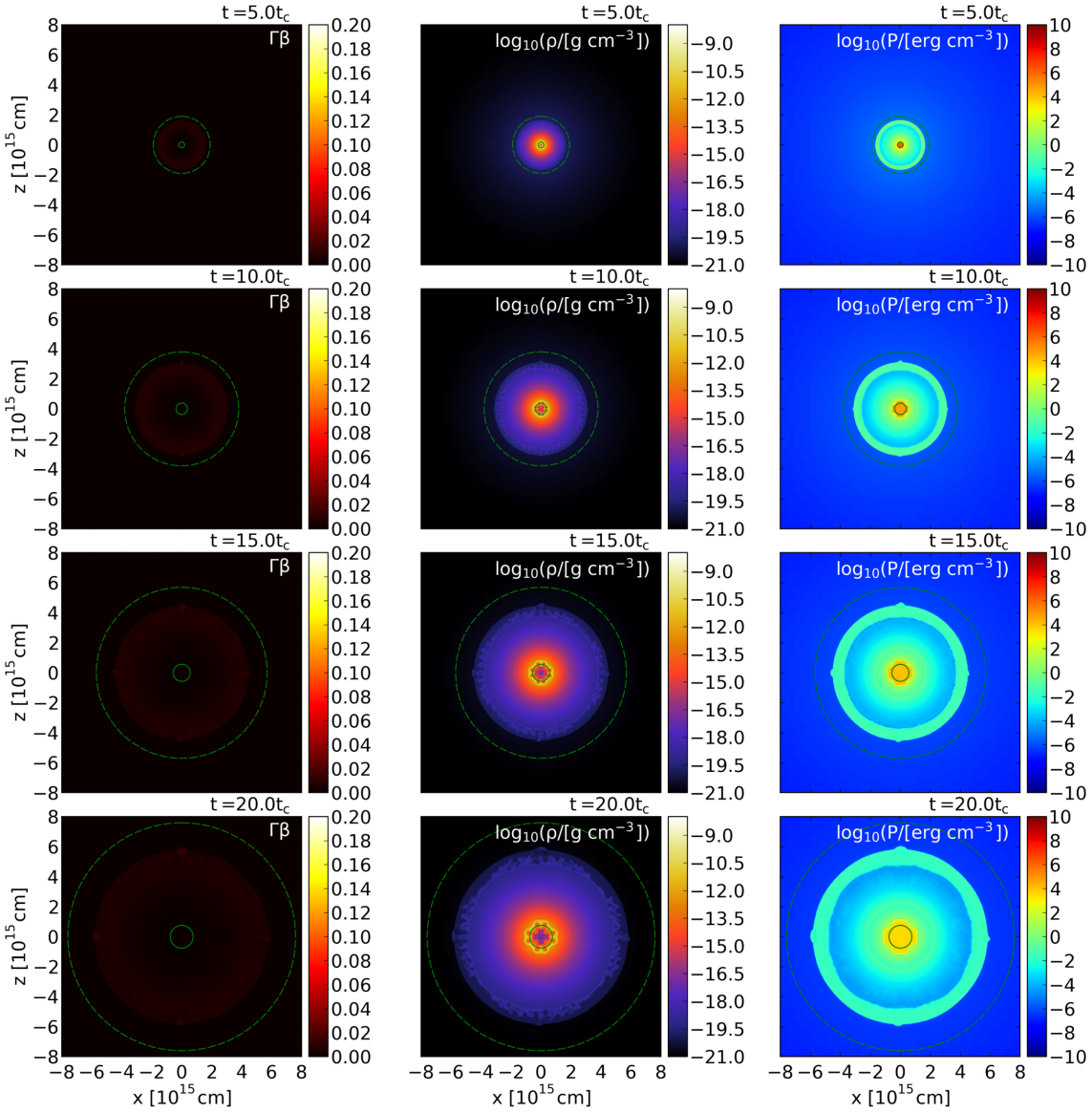

Time series of a simulation in which a central source (simple model fpr a magnetar) injects energy into expanding SN ejecta. Suzuki & Maeda (2019)

4. In the most extreme case, proto-magnetar driven MHD jets might be the sources of GRBs, with the gamma radiation produced by internal shocks or by magnetic reconnection in the jets.